PN-AAV-766
46842

CAIRO UNIVERSITY - MASSACHUSETTS INSTITUTE OF TECHNOLOGY
TECHNOLOGY AND DEVELOPMENT PROGRAM

ENHANCED ENERGY RECOVERY FROM THE EXHAUST GASES OF BASIC OXYGEN FURNACES THROUGH OPERATION AT PRESSURE.

by

Neena Suresh Shenoy
edited by David Gordon Wilson

July, 1985

PREPARED BY THE
TECHNOLOGY AND DEVELOPMENT PROGRAM
MASSACHUSETTS INSTITUTE OF TECHNOLOGY

SUBMITTED TO THE
UNITED STATES AGENCY FOR INTERNATIONAL DEVELOPMENT
CONTRACT NO. 263-0061-C-00-1001-00

SUMMARY

This theoretical preliminary-design study indicates that it is potentially possible to produce about 14 MW of net power from the exhaust gases of three small basic oxygen furnaces in the Helwan plant of the Egyptian Iron and Steel Company, Egypt.

Major changes would be required. The furnaces would require modification to, or substitution of, the suppressed-combustion type, capable of operating under a pressure of three atmospheres. The oxygen pressure would be boosted by a pressure ratio of about three, and the temperature of the compressed oxygen would be increased by heat exchange with the turbine-exhaust flow. The gases leaving the furnaces would be confined to individual ducts connected with a common duct through a one-way valve. This valve would open only when the furnace-duct pressure exceeds that in the common duct. Steam would be added to the pressurized exhaust gas to reduce its temperature. It would then flow through a single-stage reaction turbine, equipped with variable-angle nozzle vanes to enable the pressure to be maintained during flow variations. The added steam produces an increase in power output from the turbine.

The turbine exhaust gases would flow through one or more rotary ceramic heat exchangers, incorporating a neutral-gas purge stage, heating pressurized oxygen for the lances. The gases would then pass on to a waste-heat boiler, a cooler and probably a water wash before being ducted to the gas mains for use in the plant.

Such a process holds the promise of very large benefits and considerable risks. Before it could be adopted, more detailed design studies and experimental trials of increasing power should be undertaken.

PREFACE

This report is one of a series of publications which describe various studies undertaken under the sponsorhsip of the Technology and Development Program at the Massachusetts Institute of Technology.

The United States Department of State, through the Agency for International Development, awarded the Massachusetts Institute of Technology a contract to provide support at M.I.T. for the development, in conjunction with institutions in selected developing countries, of capabilities useful in the adaptation of technologies and problem-solving techniques to the needs of those countries. This particular study describes research conducted in conjunction with Cairo University, Cairo, Egypt. The analysis, conclusions, and recommendations are those of the author and do not necessarily reflect the views of the Agency for International Development.

In the process of making the TDP supported study, some insight has been gained into how appropriate technologies can be identified and adapted to the needs of developing countries per se, and it is expected that the recommendations developed will serve as a guide to other developing countries for the solution of similar problems which may be encountered there.

Fred Moavenzadeh

Program Director

ACKNOWLEDGEMENT

I would like to first thank my husband, Suresh Shenoy, for his continued support, understanding and patience during the General Electric Advanced Engineering Program and this thesis work. Thanks to G.E. for providing the funding for the Graduate program at M.I.T.. I appreciate the encouragement given by several people at G.E., especially Samir Sayegh, Chris Johnston, Les Freeman and John Stewart. My appreciation and thanks to my thesis advisor, David Gordon Wilson, whose enthusiasm and guidance made this work possible. Special thanks to Annette Papia for her friendly advice.

Neena.

DEDICATED TO MY SON NIKHIL

ADDITIONAL ACKNOWLEDGEMENT

EDITORIAL AND PROGRAM ACKNOWLEDGEMENT - This report is based on the master-of-science thesis of Neena S. Shenoy. As she acknowledges above, she was supported by a fellowship provided by the General Electric Company. She chose to do her work on a topic concerned with the Technology and Development Program joint project involving Cairo University, the Egyptian Iron and Steel Company, and Massachusetts Institute of Technology. The program is funded by a contract from the Agency for International Development, US Department of State, directed by Professor Fred Moavenzadeh at MIT. It is administered at MIT by Kevin O'Toole and Jeanne De Pass. The joint project was started by Dr. M. G. El-Maghraby at Cairo University, who drew together a highly skilled team from different departments at his own university, negotiated a successful collaboration with the Egyptian Iron and Steel Company and the Egyptian Aluminium Company, and invited MIT to be a part of the team.

Several people have contributed to the present project, in addition to those acknowledged above. Misbah Ahdab wrote an earlier master-of-science thesis on the same general topic, in which he made preliminary design studies of alternative approaches and contributed to an understanding of the metallurgy. John F. Elliott, professor of materials science and engineering at MIT, has been a generous no-cost advisor to the project, including making a ten-day visit to Egypt to make person-to-person recommendations. He also suggested many members of an advisory committee to whom we have sent draft reports and memoranda. Thse skilled and busy people have been under no obligation to respond, but in many cases they have to an invaluable extent. They include the following:

Dr. Balkrishan Agrawal
UNION CARBIDE CORPORATION
Tarreytown, NY 10591

Mr. James H. Cox
Manager, Metallurgical Processes
BETHLEHEM STEEL COMPANY
Bethlehem, PA 18106

Mr. Cecil B. Griffith
Head, Iron and Steel Processing
REPUBLIC STEEL
Independence, OH 44131

Mr. Lawrence C. Long
Corporate Director of Research
ARMCO STEEL CORPORATION
Middletown, OH 45043

Mr. David L. Peterson
Division Engineer
UNITED STATES STEEL CORPORATION
Gary, IN 46402

In addition, colleagues of members of the advisory committee were good enough to review some drafts, including C. D. Thompson of the Ironmaking Processes Group of Bethlehem Steel Corporation and D.G. White, Division Process Engineer of United States Steel Corporation.

Sabina L. Rataj and Theodosios P. Korakianitis have been invaluable during Neena Shenoy's work and in the production of this report. Neena Shenoy, author of the report, devoted a great deal of effort and expertise into her thesis to make the best possible contribution to the project.

To all of these I and my colleagues wish to express our grateful thanks.

David ordon Wilson
Mechanical Engineering Department
Massachusetts Institute of Technology
Cambridge, Massachusetts

July, 1985

CONTENTS

	PAGE
SUMMARY	1
PREFACE	2
AUTHOR'S ACKNOWLEDGEMENTS	3
EDITORIAL AND PROGRAM ACKNOWLEDGEMENTS	4,5
CONTENTS	6
NOMENCLATURE	7,8
CHAPTER 1: INTRODUCTION	11
1.1: PRINCIPLES OF MODERN STEELMAKING	11
1.2: THE HISTORY OF BASIC OXYGEN FURNACE	11
1.3: THE BASIC OXYGEN STEELMAKING PROCESS	12
CHAPTER 2: THE PRESSURIZED BASIC OXYGEN PROCESS	17
2.1: INTRODUCTION	17
2.2: EFFECTS OF PRESSURIZATION ON BOF STEELMAKING	19
.CONCLUSIONS AND RECOMMENDATIONS	21
2.3: ENERGY RECOVERY FROM PRESSURIZED BOF GASES	22
2.4: HEAT EXCHANGERS FOR THE ENERGY RECOVERY CYCLE	30
2.5: POWER-TURBINE FOR THE ENERGY RECOVERY CYCLE	31
2.6: BOF EXHAUST DUCT FOR THE PRESSURIZED CYCLE	34
CHAPTER 3: POWER-TURBINE DESIGN	36
3.1: INTRODUCTION	36
3.2: ANALYSIS OF POWER-TURBINE FOR DESIGN CYCLE	37
3.3: PRELIMINARY MECHANICAL-DESIGN OF POWER-TURBINE	40
3.4: ALTERNATIVE TURBINE DESIGN	43
3.5: CONCLUSIONS AND RECOMMENDATIONS	43
CHAPTER 4: CONCLUSIONS AND RECOMMENDATIONS (SUMMARY)	47
REFERENCES	49

NOMENCLATURE

ROMAN LETTERS

A : area; station
a : activity
B : Burner; station
B.O.F.: Basic Oxygen Furnace
C : Compressor; station; concentration; carbon; absolute velocity
C_p: Specific heat at constant pressure
E : Expander
G : Gibbs free energy
g : gravitational constant
H : enthalpy
h : enthalpy; Planck's constant
K : equilibrium constant
kg : kilogram
k : reaction-rate constant
M : atomic mass; Mega (10^6); Mach number
MWt : molecular weight
$\dot{m}$: mass-flow rate
m : mass
N : Avagadro's number
n : number of furnaces; number of moles; number of stages
O : oxygen
P : pressure
p : partial pressure
Pa : Pascal
$\dot{Q}$: heat transfer rate ($\equiv$ J/s)
q : heat transfer ($\equiv$ J/kg)
R : Gas constant; degree of stage reaction
r : pressure ratio; radius
S : entropy; speed
T : temperature
t : time
U : heat transfer per unit time
u : mean peripheral speed
V : velocity ($\equiv$ m/s)
W : watts; work; relative velocity
$\dot{W}$: power ($\equiv$J/s or watts)
w : work ($\equiv$J/kg)
X : heat-exchanger
y : mass fraction
Z : elevation

GREEK LETTERS:

ϕ: availability; flow coefficient
η : efficiency
ε: effectiveness
γ: activity coefficient; interfacial surface tension
σ: surface tension
ρ: density
ψ: loading coefficient
α: flow angles
ω : shaft speed (R.P.M.)

SUBSCRIPTS:

1,2,3,4,5,6,7 : station designators
A : added
av : average
c : compression
c.v.: control volume
e : expansion; exit
eq : equilibrium
fg : fluid-gas
g : gas
h : hub
i : ith component
L : liquid
o : total
pc : polytropic compression
pe : polytropic expansion
s : stages
st : static
t : tip
th : thermal
v : vapor
x : heat exchanger; axial
θ : tangential

LIST OF ILLUSTRATIONS

Figure 1. Historical and projected increase of turbine-inlet temperature.

Figure 2. Assumed cooling-air requirements as functions of turbine-inlet temperature.

Figure 3. Typical rotary regenerator.

Figure 4. Assumed variation of regenerator leakage flows.

Figure 5. Simple-cycle temperature-entropy and block diagrams.

Figure 6. Simple-cycle efficiency and specific power.

Figure 7. Heat-exchanger-cycle temperature-entropy and block diagrams.

Figure 8. Historical and projected increase of maximum regenerator effectiveness.

Figure 9. Heat-exchanger-cycle thermal efficiency and specific power.

Figure 10. Intercooled-cycle temperature-entropy diagram.

Figure 11. Intercooled-cycle thermal efficiency and specific power.

Figure 12. Direct-plus-inverted-cycle temperature-entropy diagram.

Figure 13. Optimum pressure ratios for inverted cycles as functions of direct-cycle pressure ratio.

Figure 14. Direct-plus-inverted-cycle thermal efficiency and specific power.

Figure 15. Summary of performance of alternative cycles.

Figure 16. Predicted compressor characteristics with contours of polytropic efficiency.

Figure 17. Turbine characteristics with contours of isentropic

Figure 18. Model of LPR engine used in NEPII calculations.

Figure 19. Turbine-inlet temperature (expressed as T') as function of percent power and speed.

Figure 20. Thermal efficiency of the LPR engine as function of percent rated power and speed.

Figure 21. Cross-sectional sketch of the LPR gas-turbine engine.

Figure 22. Variation of design-point and off-design-point thermal efficiency of four LPR engines and a typical diesel.

CHAPTER 1

INTRODUCTION

1.1 PRINCIPLES OF MODERN STEELMAKING

The first step in making steel is to reduce the iron-bearing materials (in the form of iron ore, pellets or sinter) to molten iron (pig iron) in the blast furnace. The carbon in coke is used as both the reducing agent and the fuel. The iron absorbs 3.0 to 4.0 percent of this carbon. Steel is defined as ferrous material containing less than 1.0 percent carbon, normally produced by removing the excess carbon from the molten iron taken from the blast furnace.

The excess carbon is removed by controlled oxidation of mixtures of molten pig iron and melted iron and steel scrap in steelmaking furnaces to produce carbon steels of the desired carbon content. The principal steelmaking furnaces include the open-hearth furnace, basic oxygen furnace and electric-arc furnace. All of the modern steel-making processes produce molten (liquid) steel. After the molten steel has attained the desired chemical composition in the steelmaking process, it is tapped from the furnace into a ladle and may go directly to continuous strand-casting machines or may be poured into tall, usually rectangular, molds where it solidifies to form ingots.

The preceding description of modern steelmaking might make the process appear simple but the manufacture of steel in its many product forms involves a complicated series of interrelated operations, discussed in detail in reference [1].

1.2 THE HISTORY OF THE BASIC OXYGEN FURNACE

The BOF steelmaking process was an evolutionary concept developed through the following major factors:

1. the use of nearly pure oxygen for refining molten pig iron (as distinguished from air);
2. its introduction from the above via a lance, in contrast to bottom blowing; and
3. the use of solid-bottom vessels, as a consequence of blowing oxygen from the top, decreasing maintenance costs.

The use of high-purity oxygen (i.e., 98% or better) to

refine pig iron attracted the attention of experimentalists and inventors, even in the days of Henry Bessemer more than a century ago. Bessemer could see the merit of using pure oxygen to increase steel production and excluding nitrogen to improve the quality of steel, but he could not provide the required oxygen for confirmatory trials. Karl von Linde produced the first commercial quantities of oxygen in Germany at the end of the last century. In the U.S., the first plants for oxygen were built around 1907, mainly for medical purposes. After World War II, there was a resurgent demand for civilian goods, automobiles and appliances, all requiring steel, and oxygen was available in sufficient quantity for trials in steelmaking. Process testing was conducted in open hearths by using jets of pure oxygen to melt hot scrap or by injecting oxygen from roof lances into the bath to speed up refining. These early trials showed that oxygen could increase production of steel and pay for itself in savings of fuel.

At about the same time that the roof lance was appearing in the U.S., a similar development was taking place in Austria. In Switzerland, Robert Durrer, who had long believed in converting molten pig iron to steel by the use of pure oxygen, experimented with top blowing the pig iron with pure oxygen introduced by a lance from above. According to Durrer, the first successful heats with pure oxygen were blown in March of 1948. His experiments showed that it was possible to refine iron by use of oxygen and to remove phosphorous and sulphur by the use of fluxes. Soon a team headed by Durrer and comprised of Swiss and Austrian scientists was formed to continue the development work. The joint effort was so successful that in 1952 a commercial plant with LD (Linz-Durrer or BOF) converters of 35-metric-tons capacity was opened at Linz.

From here on, oxygen use spread and the BOF came into being. The growth of the LD outside Austria was at first concentrated in North America and later in Japan, West Germany, Britain, France and Australia. At the present time the BOF is the foremost steel process in the world, with the largest vessels more than ten times the original 35-ton size.

1.3 THE BASIC-OXYGEN STEELMAKING PROCESS

The BOF comprises a vertical solid-bottom crucible with a vertical water-cooled oxygen lance entering the vessel from above, as shown in figure 1.1. The vessel is tiltable for charging and tapping. The basic-oxygen steel process

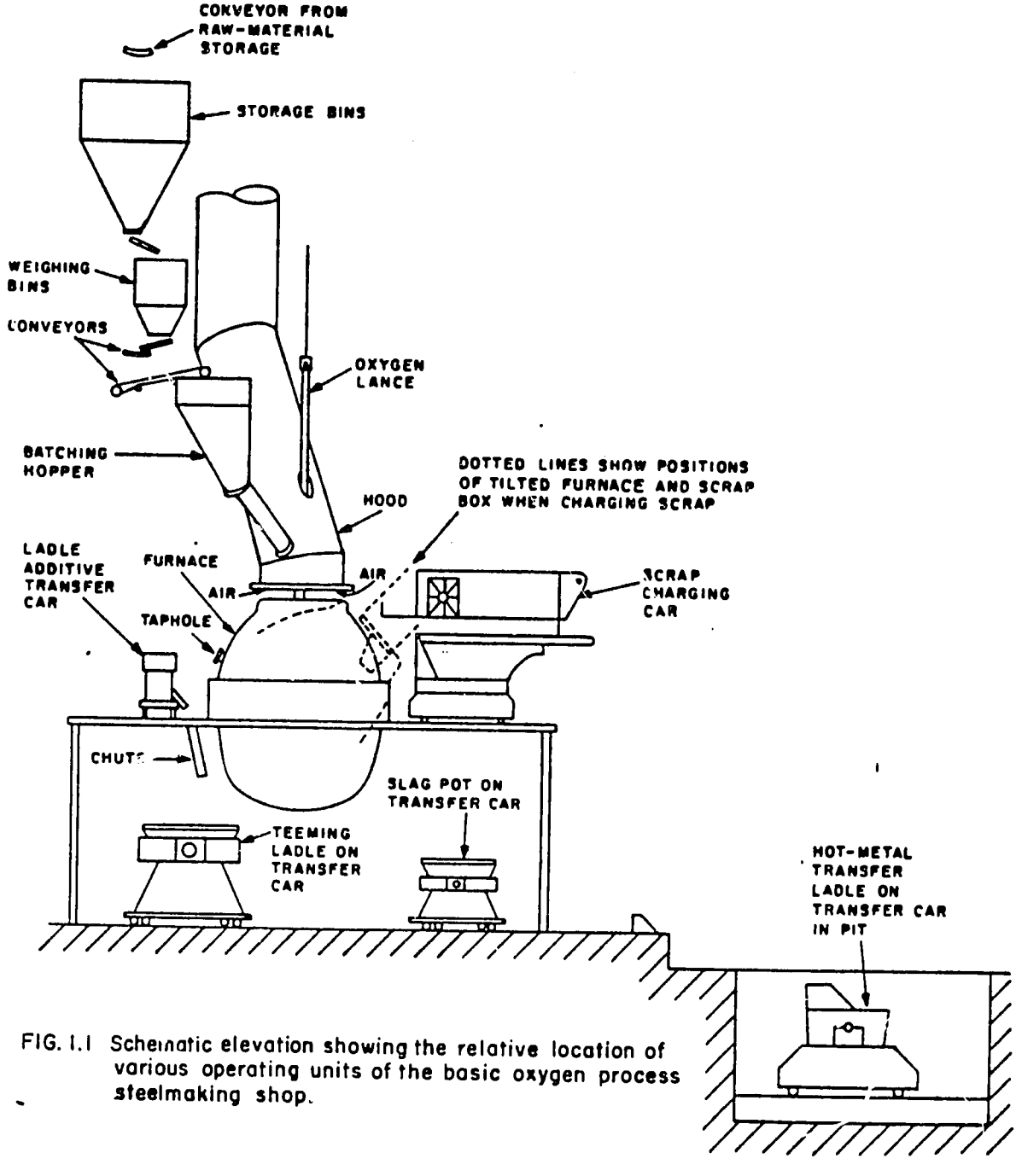

FIG. 1.1 Schematic elevation showing the relative location of various operating units of the basic oxygen process steelmaking shop.

uses pure oxygen to refine the molten iron to produce steel. Supersonic jets of oxygen are delivered through the lance, which is usually 4 to 7 feet above the horizontal bath level in the vessel. The oxygen jets are able to penetrate the floating slag and the metal, and agitate the molten iron. At first, reaction between the oxygen and the metal is localized, but rapidly intensifies with the increasing evolution of carbon-monoxide (CO) gas. The agitation and the circulation of the bath cause intimate mixing of slag and metal which contributes substantially to high-speed refining. Impurities such as silicon, carbon, manganese and phosphorous are oxidized in exothermic reactions. The combination of these impurities with oxygen generates sufficient heat not only to raise the temperature of the metal to the required level, but also to allow the use of some scrap in the charge to balance the excess heat available. Normally, 30 percent by weight of the total charge is scrap (see references [1], [2] and [7]). The exact percentages of hot metal, scrap and possibly ore pellets are determined individually for each heat by the material and heat balance to reach the desired end-point carbon and temperature. Reference [2], chapter 13, presents a complete discussion of the energy balance. These energy-balance calculations are simplified and summarized in section A.3 of Appendix A in this report.

The process steps are summarized in reference [2] as follows:

1. charging the scrap into the slightly tilted vessel;

2. charging the hot metal from the ladle;

3. righting the vessel, lowering the lance and blowing oxygen;

4. adding fluxes (or, for some grades of steel, alloying elements, if necessary) resulting in slag formation due to oxidized impurities;

5. raising the lance at the end of the blow and shutting off the oxygen;

6. turning the vessel to a nearly horizontal position and taking spoon samples and temperature data, if necessary, from the mouth opening;

7. reblowing and/or cooling if the preliminary metallurgical analysis so indicates;

8. discharging steel through the tap hole into the ladle by gradually rotating the vessel; and

9. rotating the vessel to the charging side and slagging off; i.e., dumping the slag over the furnace mouth into the slag pots.

The major advantages of the basic oxygen process include the speed of refining with pure oxygen being the only refining agent, its economy of labor and the high quality of its products.

1.4 ENERGY RECOVERY IN THE STEEL INDUSTRY.

The steel industry has the goal of utilizing some of the energy normally wasted in the furnace exhaust gases, so long as steel production is not adversely affected. Several energy-recovery systems have been developed for blast-furnace top gas. In Japan, Kawasaki Steel has achieved significant energy savings by recovery and recycling of blast-furnace exhaust-gas energy in the form of preheating the blast air and the scrap and of generating steam (reference [3]). In the U.S., energy recovery from blast-furnace slag for preheating blast air has been proposed (reference [4]). Fewer feasible energy-recovery systems have been proposed for BOF exhaust gases. In the late fifties, Philbrook (reference [5]), showed that carbon monoxide discharged from the BOF and used to heat the charge would permit increasing the percentage of scrap in the charge. Numerous attempts have been made to use more scrap but all have proved to be expensive processes. An exhaust-gas energy-recovery system to generate power and add more scrap to the BOF is proposed in the succeeding chapters.

CHAPTER 2

THE PRESSURIZED BASIC OXYGEN PROCESS

2.1 INTRODUCTION

The waste gas emitted from a conventional BOF is typically composed, according to reference [18], of 95% carbon monoxide (CO) and 5% carbon dioxide (CO_2). In most such BOF plants currently in operation, the combustible CO in the furnace gas at high temperatures is burned with excess air drawn into an open hood. Carbon-monoxide combustion raises the gas temperature at the hood entrance to around 3000°K. Clearly, this gas flow contains large amounts of recoverable energy (availability) but little is in fact recovered. Some of this heat is absorbed by water required to cool the hood and is converted to steam for plant use, and some goes to evaporate the water that is injected into the exhaust duct to cool the gases. Also a typical BOF-waste-gas handling system [reference [2], chapter 10] consumes about 2000 kW per furnace to power induced-draft fans, and also generates large quantities of sludge; thus energy is expended at a high rate to dispose of a high-energy gas flow.

Some efforts to recover a portion of this high-quality energy, in addition to the steam raised from the cooling water, have been made. Also, the chemical energy in the BOF gas is sometimes recovered through the suppression of combustion at the furnace mouth: a skirt (seal) is lowered around the furnace which restricts airflow into the combustion zone (reference [20]). By limiting air infiltration only about 10% of the CO in the waste gas is allowed to combust; gas is collected at a lower temperature and with considerable chemical potential.

Several researchers have discussed pressurization of the basic oxygen process, including reference [7]. The advantages of pressurizing the BOF and the effects of pressure on chemical reactions in steelmaking are discussed next.

In section 2.3, a low-pressure thermodynamic cycle is proposed to recover energy from the pressurized BOF.

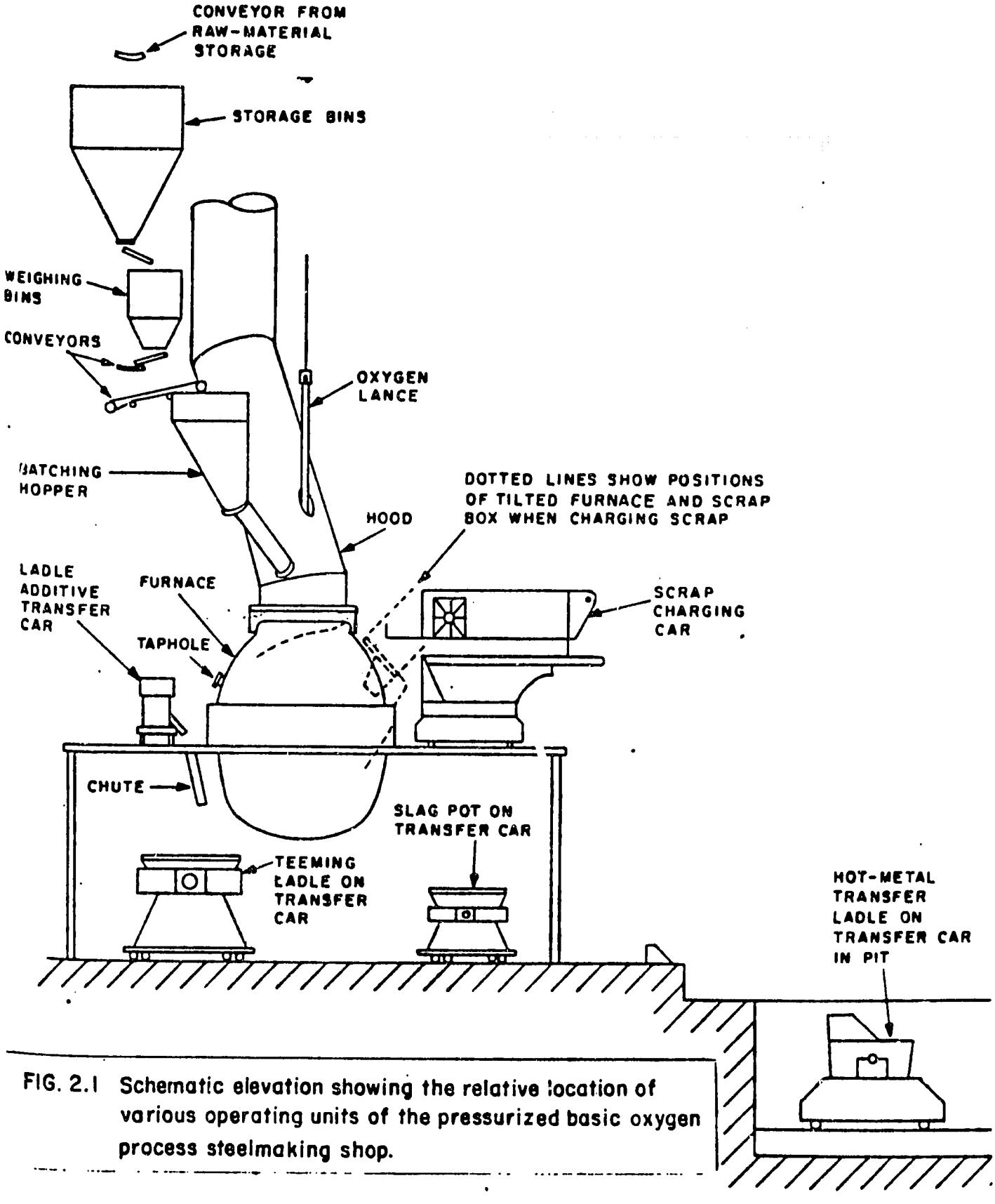

FIG. 2.1 Schematic elevation showing the relative location of various operating units of the pressurized basic oxygen process steelmaking shop.

The available energy [in Btu/lbm or J/kg] in the exhaust gas can be increased by application of pressure to the BOF system. As seen in equation (B.34) of Appendix B, if both the conventional and the pressurized systems are at the same temperature, pressurization increases availability. The objective is also to recover as much uncombusted CO as possible from the furnace gas for its calorific value. A closed-hood system as shown in figure 2.1 has to be used to pressurize the BOF and hence infiltration of air into the hood would be made negligible. This would prevent CO combustion above the furnace. The resulting reduction of temperature from that of an open hood could make the exhaust system potentially longer lasting. Also this closed, high-pressure gas system could be much smaller than the conventional open system or a closed, unpressurized system. The diameter of the exhaust duct is estimated in section 2.6 as 1.06m for furnaces of the size used in the Helwan plant; this is only about one-fourth of the typical duct size of 4.4m as given in reference [1] for an open system.

Therefore pressurization of the BOF could provide surplus energy, decrease the size of the exhaust-gas system and make it potentially longer lasting with lack of combustion.

2.2 THE EFFECTS OF PRESSURIZATION ON CHEMICAL REACTIONS AND REACTION RATES IN THE BOF STEELMAKING PROCESS

The chemistry of steelmaking is made complex by the numerous reactions and surface phenomena occurring during refining. BOF pressurization adds to this complexity. No experimental data seem to be published on pressurized operation. Only a theoretical paper by Stone, reference [7], on the LD (BOF) process at high pressure has been published. Several theoretical effects of pressure on BOF operation are analyzed in Appendix A and the results are discussed in this section.

Pressurization will promote CO_2 formation in the furnace from the CO- and oxygen-combustion reactions, equation (A.10). This follows from Le Chatelier's principle: the pressure increase will favor the side of the reaction with the lower total number of moles. However, the rise in temperature due to the the promoted CO combustion

in the furnace could in turn suppress this exothermic reaction. With the carbon in molten iron having a negligible volume compared to the gases in equation (A.15), pressurization will favor dissociation of CO in this exothermic reaction. Due to the increase in pressure of CO, the partial pressure of oxygen would increase, as shown in equation (A.16). This in turn will increase the oxygen potential which could become high enough to oxidize the iron. As discussed in Appendix A, removal of impurities like silicon, manganese and phosphorous could be promoted by BOF pressurization.

The reaction rates could increase or decrease with increasing pressure depending on the volume of the final state being smaller or larger than the volume of the initial state (see Appendix A, equation (A.37). This suggests that the reaction rate for CO2 formation increases, while that for CO_2 formation decreases with increasing pressure. However, significant changes in reaction rates are reported in reference [10] to occur only at high pressures - of the order of 60 atmospheres - and so that at a pressure of three atmospheres proposed for pressurizing the BOF, the change in reaction rate could be negligible.

Nucleation of bubbles (like carbon boil) within the bath is required for refining steel. However, the rate of furnace operation is found to be limited (reference [2], chapter 5) by the start time required for nucleation of these bubbles within the bath. As discussed in Appendix A, pressurization would lower the amount of superheat required for nucleation to initiate and hence the carbon boil could start sooner.

A large surface area is required for the rapid rates at which reactions occur in the BOF as seen in equations (A.43) and (A.44). The areas of the order of vessel dimensions are not sufficient to account for the very high observed rates of reaction in the BOF. Current theories (reference [2]) rely heavily on the phenomena of emulsions and foams to account for the large interfacial area between the two phases, like the slag/gas interface. As discussed in section A.4, emulsion could be favoured by pressurization and the resulting increase in interfacial area could enhance the rapid rates of reaction in the BOF.

Conclusions and Recommendations

The furnace gas in the conventional BOF is reported at the beginning of this section to be 95% CO and 5% CO_2. In general, pressurization would affect CO_2 and CO formation but only experiments can predict the amounts of CO and CO_2 in the furnace-gas at a pressure of 3 atmospheres. Based on the 5% increase in CO_2 at 10 atmospheres postulated by reference [7], at the lower pressure of 3 atmospheres, the amount of CO_2 in the furnace gas could increase by less than 5%. This would mean the pressurized furnace gas at three atmospheres is between 90% to 95% CO and between 10% to 5% CO_2. Even though the higher amount of CO could be obtainable for energy benefits, in the following section 2.3, the furnace gas is assumed to be 90% CO and 10% CO_2 for energy-recovery calculations.

Pressurization of the BOF is recommended based on the following findings.

1. If there is no further combustion of CO in the closed, pressurized furnace, that is about 95% CO is obtained, then the objective to obtain as much uncombusted CO as possible and increase life of exhaust system would be achieved.

2. If CO_2 formation in the BOF is promoted due to pressurization, more scrap could be added to absorb the heat liberated. So any temperature rise that could have occurred is prevented. This would mean the exothermic reactions for CO_2 formation would not be suppressed but nor would the exothermic reaction for CO formation and the potential for the exhaust system to last longer may not be affected. Again, only experiments can predict the exact CO/CO_2 ratio at a pressure of 3 atmospheres.

3. The size of the closed, pressurized exhaust duct will decrease significantly from the size of the unpressurized duct by an estimated seventy-six percent.

The oxygen blow in the pressurized BOF would have to be closely controlled:

1. to prevent over oxidation of iron that could be initially oxidized due to the increased oxygen potential; and
2. to prevent blowing excess oxygen that would facilitate further combustion of CO to CO_2 in the furnace.

At a low pressure of three atmospheres, the change in reaction rates in the BOF could be negligible. The phenomena of nucleation, emulsification and foaming in the BOF and their effects on steelmaking are relatively new topics under investigation. It would be unrealistic to draw any firm conclusions on the effects of a pressure of three atmospheres on these complex phenomena.

The CO that can be recovered from a closed system has a calorific value (L.C.V.) of 318 Btu/cu.ft. (2829 kg.cal/cu.m) (reference [19]). As discussed earlier, if the amount of CO in the furnace gas decreases due to pressurization, at three atmospheres the decrease may not significantly affect the availability gains by pressurization, i.e. even if:

$$(Kg\,CO)_{pressurization} < (Kg\,CO)_{conventional}$$

CO yield under pressurization § CO yield unpressurized (2.1)

the following equation may be true:

$$(\phi)_{pressurization} \times (Kg\,CO)_{pressurization} > (\phi)_{conventional} (Kg\,CO)_{conventional} \quad (2.2)$$

It is recommended that equations (2.1) and (2.2) be verified at a pressure of 3 atmospheres.

2.3 ENERGY RECOVERY FROM PRESSURIZED BOF EXHAUST GASES

A low-pressure thermodynamic cycle for energy recovery from exhaust gases of a pressurized basic oxygen furnace in a steelmaking plant is set up in figure 2.2 and represented on a T-S diagram in figure 2.3. The cycle and the analytical results from Appendix B, section B.2, are discussed in this section.

In this system, the furnace [B] would be initially charged with hot metal, steel scrap and alloying elements just as in a conventional BOF. Then the furnace would be sealed, possibly by one of the methods in appendix 4 of reference [4]. The oxygen to be blown into the BOF is compressed for delivery at a higher pressure. As discussed later in this section, the cycle formed by the added oxygen compressor, the BOF, and the expansion turbine to be fitted

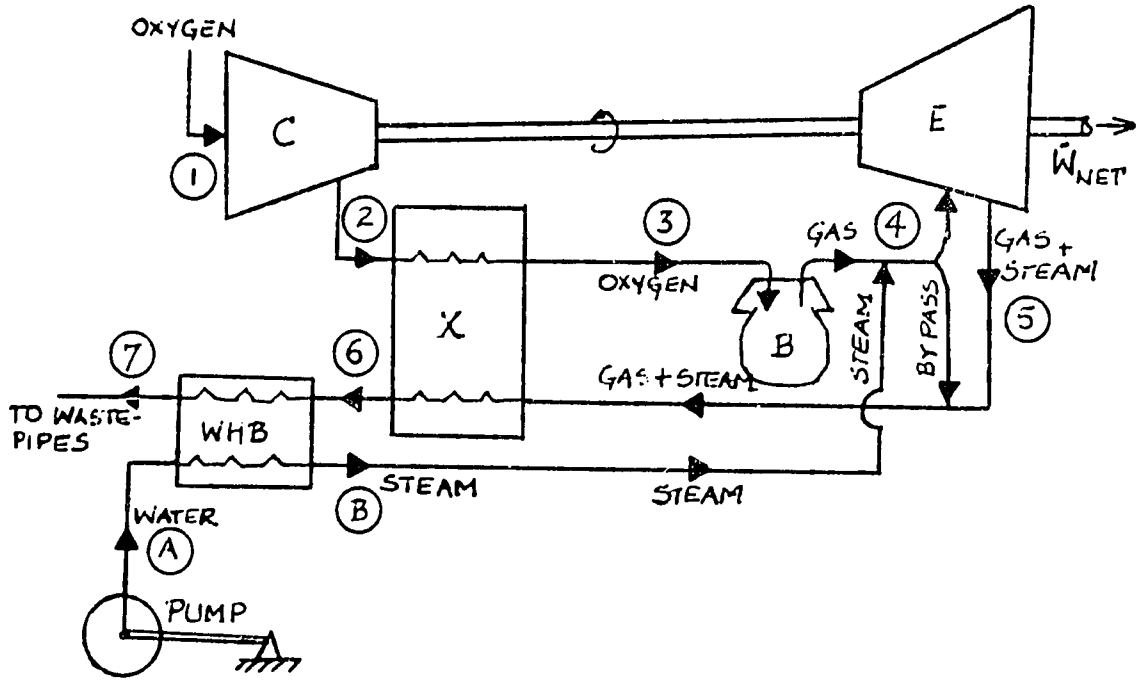

FIGURE 2.2 CYCLE FOR ENERGY-RECOVERY FROM EXHAUST GASES OF THE BASIC OXYGEN STEELMAKING FURNACE

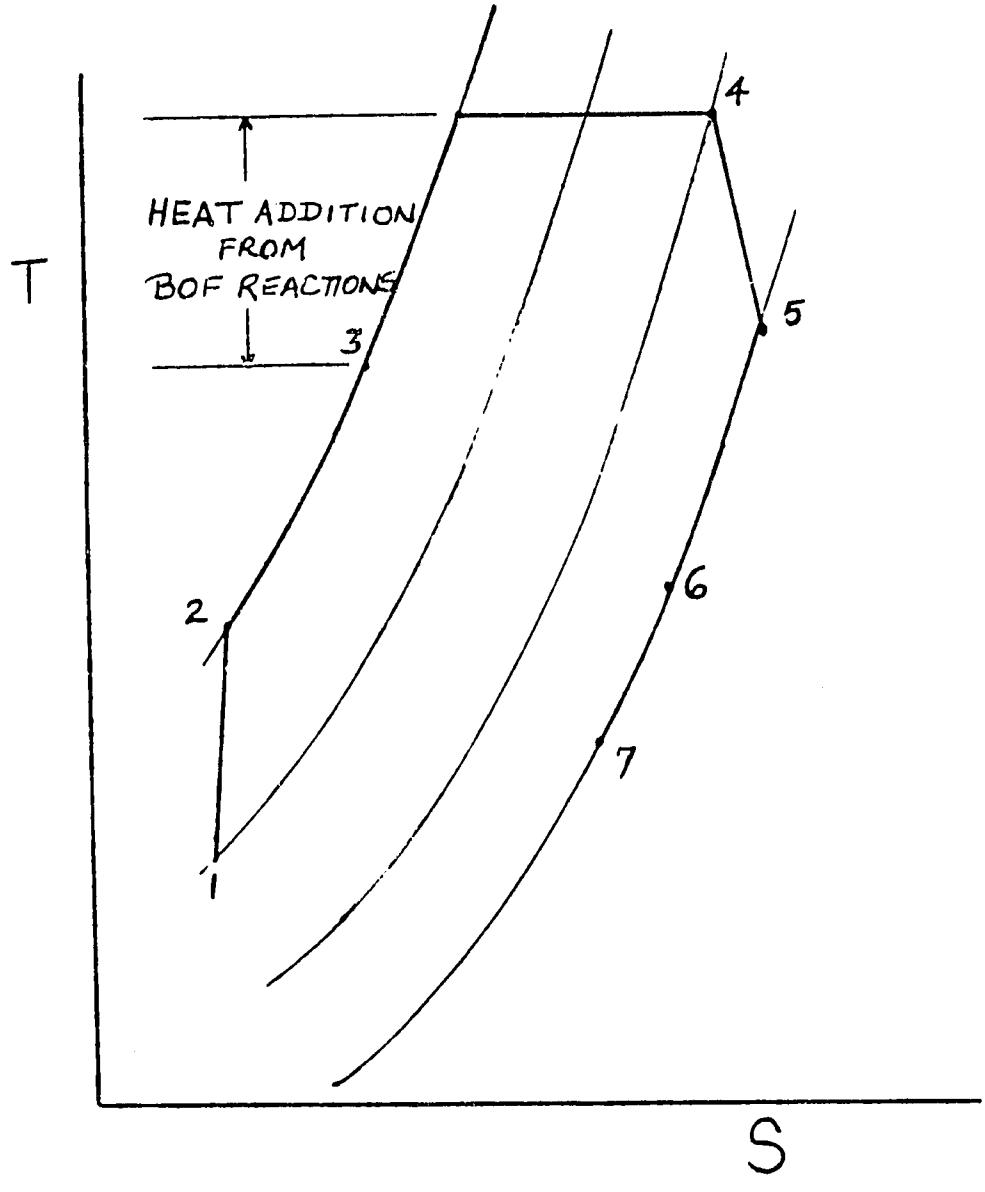

FIGURE 2.3 TEMPERATURE-ENTROPY DIAGRAM FOR ENERGY-RECOVERY CYCLE OF FIGURE 2.2

downstream has an optimized pressure ratio of 3. The stagnation pressure of the oxygen upstream of the delivery lance in a conventional BOF is obtained from reference [2], chapter 8, to be about 135 psig or 149.7 psia (1.03 MPa) and the stagnation temperature to be 100F or 310.78K. The oxygen is assumed to be at these corditions before it enters the compressor [C] in figure 2.2. At a given pressure ratio, the power required to operate the oxygen compressor is determined by methods in Appendix B.

The oxygen is then supplied to the pressurized BOF where the pressure is above atmospheric. The supply oxygen lance would have to be modified to deliver the compressed oxygen at a higher pressure in the BOF.

The exhaust gas produced from the BOF during the oxygen blow is assumed to be 90% carbon-monoxide and 10% carbon dioxide and at a temperature, T_{04}, of 1590K (=2400F). This gas is to be passed through a power turbine [E], possibly attached to an electric generator. However, gas at this temperature would require that the turbine be cooled. While aircraft turbines and their derivatives operate with much higher turbine-inlet temperatures, it is felt that for the present application uncooled turbines should be used, even at some sacrifice of power recovery, because they will presumably give higher reliability. We propose, therefore to inject steam to lower the turbine-inlet temperature, T_{04}, to 1200K (=1700F), a temperature tolerable by currently available turbine materials. The added mass flow due to the steam produces an increase in the power output by the turbine. Several possible power-turbine configurations are considered. The power turbine recommended for a low-pressure cycle is given in section 2.5 of this chapter. Other power-turbine configurations are presented in chapter 3. The mass-flow rate of steam required to cool the gas temperature to 1200K and the net power output by the turbine are determined in Appendix B.

The exhaust from the turbine is then passed through a heat exchanger [X] where heat is transferred from the exhaust stream to the compressed-oxygen stream. The flow exiting the heat exchanger is still at a temperature high enough to generate the steam, required for injection, by means of a waste-heat boiler. Some possible heat-exchanger configurations are briefly presented in section 2.4 of this chapter. Several cyle studies for varying pressure ratios

are performed based on methods in Appendix B. The results are summarized in tables I and II for steam-injected cycles and non-steam-injected cycles respectively.

Pressure-Ratio Optimization

Attempts were made to optimize the pressure ratio for the pressurized BOF cycle in figure 2.2, based on:

maximum net power, $\dot{W}_{net}$;

maximum thermal efficiency, η_{th} ;

requirement of a single-stage, low-cost power-turbine; and

requirement of low pressure ratio in the BOF so that the chemical reactions are not affected significantly.

A low-pressure ratio range of 1.5 to 6.0 was initially specified based on earlier work (Misbah and reference [4]). The net power output as defined in equation (B.36) of Appendix B increased with increasing pressure ratio, as seen in TABLE I. This could be as expected for a heat-exchanger, or CBEX, cycle (reference [14], fig. 3.6, pp116). As shown in Appendix B, the maximum power output is calculated to occur at an unrealistic pressure ratio of 84. Similarly, the thermal efficiency as defined in equation (B.35) increased with increasing pressure ratio. However, to fulfill specification (3) where a single-stage turbine is required, it is found that for a pressure ratio of 4.0, a two-stage turbine is required. Hence a pressure ratio of 3.0 was chosen, as also being low enough to have little significant effect on the BOF process.

Conclusions and Recommendations

It is recommended that the pressurized BOF cycle at a low pressure ratio of 3.0 with steam injection (case C, TABLE I) be considered for future incorporation into the Helwan plant in Egypt perhaps in an experimental program. The cycle could be designated for pure power generation with essentially all steam generated by the boiler recycled through the power-turbine. This type of cogeneration has

TABLE I
ENERGY RECOVERY CYCLE (WITH STEAM INJECTION)[3]

CASE	r_c	r_e	T_{02} [K]	T_{03} [K]	T_{05} [K]	T_{06} [K]	$\dot{m}_{steam}$ kg/s	POWER OUTPUT W_{net}, [MW]
A	1.50	1.35	352.73	942.75	1139.42	970.14	4.69	4.60
B	2.00	1.80	385.59	909.23	1083.78	931.43	4.69	8.91
C	3.00	2.70	436.35	865.22	1008.17	881.36	4.67	14.42
D	4.00	3.60	475.79	837.04	957.46	848.72	4.64	17.92
E	6.00	5.40	536.62	800.62	888.62	808.30	4.78	22.43

SPECIFICATIONS COMMON TO ALL CASES:

T_{01} = 310.78 K
T_{04} = 1199.82 K (1700 C)
T_{07} = 425 K (150 C)
ε_x = 0.75
$\dot{m}_{gas}$ = 42.6 kg/sec
$\dot{m}_{o2}$ = 25.33 kg/sec
η_{pc} = 0.90 = η_{pe}

$\dot{m}_{steam}$ increases at r_c = 6.0 because the incoming steam is assumed to be at 450 K and 6atm vs 425°K and respective pressures for other cases (see equations (B.93) of Appendix B). This is done to obtain superheated H_2O at 6atm.

TABLE II

ENERGY RECOVERY CYCLE (WITHOUT STEAM INJECTION)

CASE	r_c	r_e	T_{02} [°K]	T_{03} [°K]	T_{05} [°K]	T_{06} [°K]	NET POWER OUTPUT $\dot{W}_{net}$, [MW]
F	1.50	1.35	352.73	1361.23	1473.28	951.81	5.24
G	2.00	1.80	385.59	1306.79	1409.15	929.66	7.89
H	3.00	2.70	436.35	1209.74	1295.67	892.22	12.68
I	4.00	3.60	475.79	1146.15	1220.63	869.73	15.69
J	6.00	5.40	536.62	1062.12	1120.51	841.70	19.38

SPECIFICATIONS COMMON TO ALL CASES:

T_{01} = 310.78° K

T_{04} = 1588.72° K (2400° C)

T_{01} = 425 K (150° C)

ε_x = 0.90

$\dot{m}_{gas}$ = 42.6 kg/sec

$\dot{m}_{c2}$ = 25.33 kg/sec

η_{pe} = 0.90 = η_{pc}

been done before by using the Cheng cycle (reference [16]) at installations in San Jose State University and the Sunkist Growers in California. The result is reported as a system that combines operating flexibility and mechanical simplicity. In the proposed pressurized BOF cycle (case C in TABLE I) the operating parameters permit using standard, proven industrial components except for the pressurized furnace itself and the heat exchanger. This latter would probably be ceramic, because of the temperatures involved, either fixed-surface or rotating regenerator. Because of the use of hot combustible gases on one side and oxygen on the other a nitrogen (for example) blow-down sector would probably be required for a rotary unit. The three or more BOFs in the Helwan plant could be connected by a single duct to the power turbine. The resulting large mass flow rates out of the BOFs could warrant sizing the turbine system to handle a fraction of peak output and bypassing some of the flow past the turbine to the waste-heat boiler to generate surplus steam. This would, however, decrease the cycle power generated and what combination of bypass and turbine flow will have to be an economic decision. A possible combination is presented in section 3.3 of chapter 3.

The rise in temperature of the oxygen due to compression and the heat exchange could increase the heat liberated in the BOF and allow for more scrap usage, consequently, increasing steel production (see Appendix A, section A.3). If the additional scrap is to be charged during the oxygen blow it is suggested that this be done through a modified flux-chute. The feasibility of adding scrap this way has to be investigated.

The turbine inlet temperature, T_{04} , could be made to remain constant by adjusting the mass flow rate of steam injected. This in turn would eliminate fluctuating thermal loads and increase turbine life. Also, reducing turbine inlet temperature from 1588°K to 1200 K would add to life. In aircraft engines it has been estimated that for every 30 K reduction in turbine inlet temperature, the engine life is doubled.

Finally, it is recommended that the oxygen compressor be designed for a pressure ratio of 3 and that the cycle efficiency be evaluated based on availability (see equation (B.37)) for a low-pressure range.

2.4 HEAT EXCHANGERS FOR THE CYCLE

This section briefly discusses analyses of the heat exchanger and waste-heat boiler involved in the pressurized BOF cycle.

As shown in Appendix B, the temperature of the oxygen leaving the heat exchanger, T_{03} , is determined from the specified effectiveness of the heat exchanger. By means of an energy balance, equation (B.63), and the calculated T , the exit temperature, T_{06} , of the turbine gases leaving the heat exchanger is determined. A similar energy balance is performed on the waste-heat boiler for a specified gas exit temperature, T_{07} , of 425K and the mass flow of steam provided by the boiler is obtained.

The pumped water enters the boiler as a subcooled liquid, subsequently rises in temperature to its boiling point and exits the boiler as superheated steam for injection. Throughout the two-phase region the temperature is assumed to stay constant and figure 2.4 illustrates the temperature distribution in a counter-flow boiler analyzed in Appendix B. At a saturation temperature of 408K for boiling to initiate at 3 atmospheres and with T_{07} = 425 K, an adequate "pinch point" of greater than 17° K is obtained (see figure 2.4).

The heat exchanger by which the heat transfer between the turbine exhaust and the compressed oxygen is effected has a severe duty. In general, heat exchangers may be divided into fixed-wall and switching-wall types. The fixed-wall variety includes conventional tubular, tube-fin and plate-fin types. They must be ruled out of contention, with one proviso, because the temperatures involved are higher than could be withstood by any metals from which heat-exchanger surfaces could be made. The exchangers being evaluated and tested, and if these are successful they would be obvious candidates for the exhaust-gas-to-oxygen heat exchanger.

The steel industry has, however, used switching-wall heat exchangers for many years (ref. 22). The Cowper or "hot" stoves are of this type. The switching is relative: in the Cowpers the gas flow is switched among several chambers full of ceramic "checkerwork". The hot gases heat

up the checkerwork in one chamber and are then switched to another chamber while cool gas is fed in reverse flow through the first chamber, and so on. The electric-power industry has used rotary air preheaters for many years, and a version that is almost universal on automotive gas turbines and which uses a rotating ceramic matrix is shown in figure 2.5. The heat-exchanger matrix spans two adjacent ducts, one carrying the hot turbine exhaust and the other the oxygen flow to be heated. In application to this duty it might be necessary to incorporate purging flows within the seal area if the reactions of the small quantities of carried over oxygen and exhaust gas appear to be harmful.

Recommendations.

The rotary ceramic-matrix heat exchanger (developed initially by Corning Glass) appears to have appropriate characteristics for the duty of heating the oxygen from the waste heat in the turbine exhaust. The handling of oxygen requires extreme care in all circumstances, of course, and it could well be decided that oxygen preheat be deferred until a later stage and that injection of relatively cool oxygen be injected into the BOFs initially;. There would be a small reduction of shaft power from the turbine. This could be restored by adding the heat exchanger at a later stage in plant development.

The temperatures obtained (figure 2.4) for the waste-heat boiler are within those for proven, industrial boilers. A specific configuration for the boiler to match the temperatures has to be obtained in the future.

References [4], [21] and [22] provide detailed analysis and several common available configurations of heat exchangers.

2.5 POWER TURBINE FOR THE ENERGY-RECOVERY CYCLE

The mean-diameter velocity diagram of a fifty-percent-reaction, high-work turbine has been chosen for the steam-injected energy-recovery cycle with a pressure ratio of three. A detailed design analysis and discussion of this turbine is provided in sections 3.1, 3.2

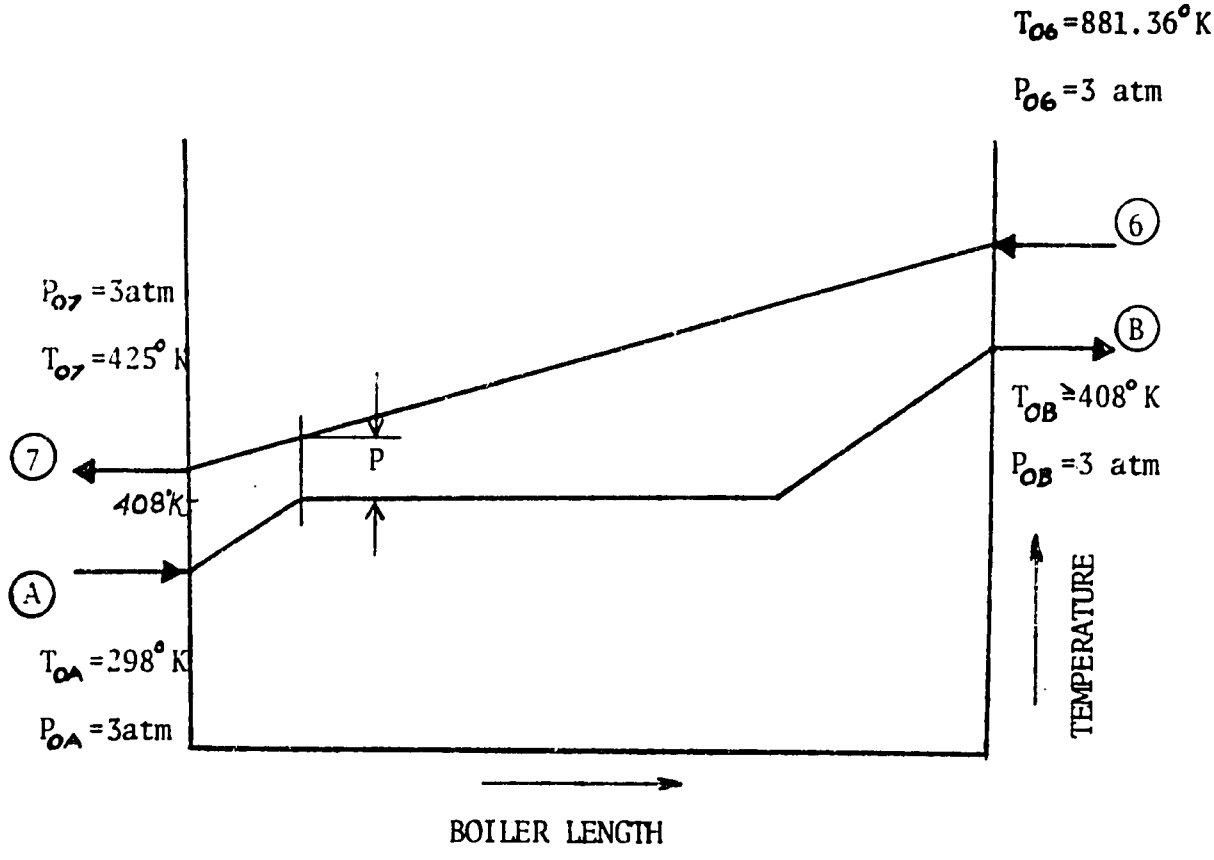

FIGURE 2.4 REPRESENTATION OF TEMPERATURE DISTRIBUTION IN A COUNTERFLOW WASTE-HEAT BOILER.

P = PINCH POINT.

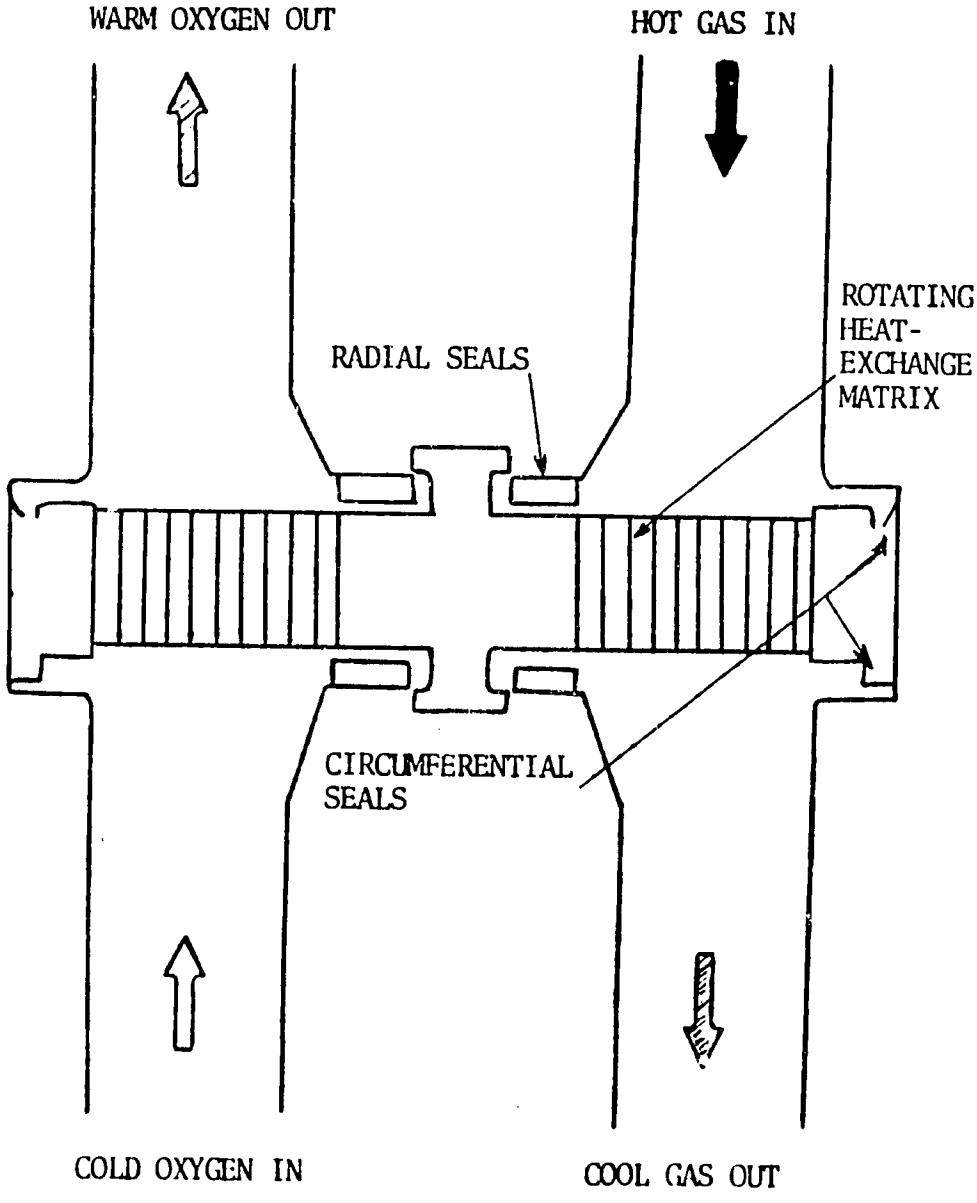

FIGURE 2.5 OPERATION OF THE ROTATING REGENERATOR, REFERENCE [21]

and 3.3 of chapter 3. This turbine is about five feet (1.50m) in diameter with rotor blades about six inches (152mm) in height. It is designed to handle about sixty-five percent of the peak gas flow exhausting from the three BOFs of 80-ton capacity each at the Helwan plant in Egypt. The shaft speed for this power turbine is about 6800 R.P.M. and the flow is subsonic at turbine-rotor inlet.

If this turbine is required to handle a different amount of peak gas flow, the design sequence would be as follows.

1. Choose the combination of bypass proportion and the minimum delay to be specified between startings of the BOFs, Δt_s. See section 3.3 for an example combination.

2. Using figures 3.2 and 3.2A and equations (3.20), obtain the peak gas flow through the turbine, $\dot{m}_{TG}$.

3. Determine the mass-flow rate of steam required based on $\dot{m}_{TG}$ in (2) and equation (B.93). Then the total peak mass-flow rate through the turbine would be,

$$(\dot{m}_{T_{peak}} = \dot{m}_{TG} + \dot{m}_{\substack{steam \\ required}})$$

4. Size the turbine as i· sections 3.3 and 3.4 and if necessary use reference [14] chapter 7 for further design of turbine components, especially the blades

2.6 BOF EXHAUST DUCT FOR THE PRESSURIZED CYCLE; P = 3atm., T = 1199.82 K

From equation (B.103) in Appendix B, the mass-flow rate is given by

$$\dot{m} = \rho VA \qquad (....2.3)$$

With

$\dot{m}$ = 132.0 kg/s (see equation (3.20);
ρ = 0.65 kg/m (see equation (3.23); and
V = C_X = 229.46 m/s (see equation (3.14);

the area of flow is determined from equation (2.3) to be

$$A = 0.89\ m^2 = \frac{\pi D_c^2}{4} \qquad (....2.4)$$

Therefore, the diameter of the duct, D , is calculated to be

$$D = 1.06 \text{ meters} \qquad (....2.5)$$

So the diameter of the exhaust duct of a furnace pressurized to 3atm is 1.06m. In the conventional BOF system, the exhaust duct (hood) is typically about 4.4m in diameter (reference [1] pp488-489). The gas temperature will also be considerably lower (2400 F or 1316 C vs 4940 F or 2726 C) so that the cost of the pressurized duct should be considerably less than the unpressurized duct. Both require water cooling in the uninsulated state. The pressurized duct could be internally insulated with firebrick, but as we wish to reduce the gas temperature by steam injection, the use of water (or steam) cooling for the duct seems to be a better choice.

CHAPTER 3

POWER-TURBINE DESIGN

3.1 INTRODUCTION

A turbine stage consists of a row of fixed blades or nozzles followed by a row of moving blades. Blading can be categorized as impulse or reaction. In an impulse turbine all the static-pressure drop occurs in the nozzle and the rotor converts kinetic energy into shaft work. In a pure reaction turbine, the entire pressure drop occurs in the moving-blade passage. So the moving blade acts as a nozzle and the only purpose of the stationary blades is to direct the fluid into the moving blades at the proper angle. The most commonly used turbine is the one with 50% reaction where half the enthalpy drop occurs in the nozzle and the other half in the rotor.

The work done by a rotor in a turbine stage can be represented by Euler's equation as:

$$\frac{\dot{W}}{\dot{m}} = \frac{1}{g_c}\left[u_1 C_{\theta_1} - u_2 C_{\theta_2}\right] \qquad (3.1)$$

where u_1 is the rotor peripheral speed at the radius of flow entry; u_2 is the rotor peripheral speed at the radius of flow exit; and C_{θ_1} and C_{θ_2} are the tangential flow velocities at rotor entrance and exit respectively.

For an adiabatic flow with negligible changes in potential energy, equation (B.4) in Appendix B can be written as:

$$\dot{W} = \dot{m}\left[h_{01} - h_{02}\right] \qquad (3.2)$$

where h_{01} and h_{02} are total enthalpies at rotor entrance and exit respectively.

By combining equations (3.1) and (3.2) we get:

$$g_c\left[h_{02} - h_{01}\right] = u_2 C_{\theta_2} - u_1 C_{\theta_1} \qquad (3.3)$$

or, assuming the change in radius of the mean flow is negligible, equation (3.3) becomes:

$$g_c\left[h_{02} - h_{01}\right] = u\left[C_{\theta_2} - C_{\theta_1}\right] \qquad (3.4)$$

This equation is used in interpreting velocity diagrams to obtain relative enthalpy change in a stage design.

There are three parameters that completely specify a stage velocity diagram and are discussed in reference [14]. The three parameters are the work coefficient, the flow coefficient and the stage reaction. The work or loading coefficient. ψ , is defined as:

$$\psi \equiv \frac{g_c \Delta h_{o\,stg}}{u^2} = \frac{\Delta C_{\theta\,stg}}{u} \tag{3.5}$$

The flow coefficient, ϕ, is defined as:

$$\phi \equiv \frac{C_x}{u} \tag{3.6}$$

where C_x is the axial flow velocity.

The geometrical relationship of the difference of tangential flow velocity to blade peripheral speed is given by the stage reaction, R_n, defined as:

$$R_n \equiv \frac{\Delta h_{static,\,rotor}}{\Delta h_{o,\,stage}} \approx 1 + \left[\frac{C_{\theta 2} - C_{\theta 1}}{2u}\right] \tag{3.7}$$

for streamlines with constant axial velocity.

3.2 ANALYSIS OF POWER TURBINE FOR DESIGN CYCLE

Based on these parameters and the given specifications, a preliminary design of the power turbine is performed as follows.

Specifications: Reaction Turbine (Case T1)

$$u_{max\ mean} = 500\ m/s$$
$$\psi = 1.75$$
$$R_n = 50\%$$
$$\text{hub-to-tip ratio}, \frac{r_h}{r_t} = 0.8$$
$$\text{rotor inlet flow absolute velocity angle}, \alpha_0 = 70^\circ$$

Calculations: The velocity diagram is represented in figure 3.1 and it is symmetrical since a 50% reaction turbine is specified.

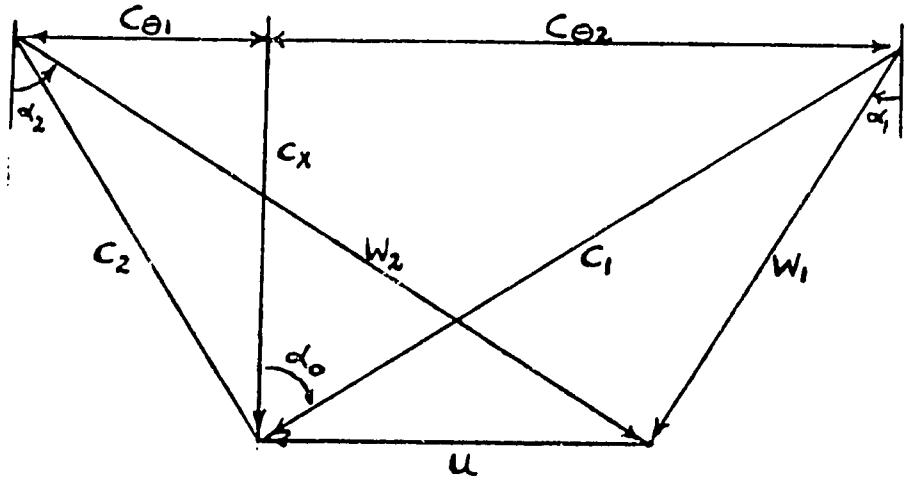

FIGURE 3.1: TURBINE-STAGE VELOCITY DIAGRAM
HIGH-WORK TURBINE (ψ = 1.75)

From equation (3.5) the maximum change in stage enthalpy is obtained as:

$$\Delta h_{0STG\,max} = \frac{(1.75)\,(500\ m/s)^2}{1\ \frac{Kg\text{-}m}{S^2}\ \frac{1}{Newton}\ \frac{1\text{-}Newton\text{-}m}{J}} = 437.5\ \frac{KJ}{Kg} \qquad (3.8)$$

For the design cycle, the turbine work is obtained from Appendix B, equation (B.57) as:

$$W = 367864.77\ J/kg \quad \text{or} \quad 367.86\ KJ/Kg \qquad (3.9)$$

and this equals the total enthalpy change across the turbine. Therefore the number of stages of expansion required are obtained as follows:

$$\eta_s = \frac{367.86\ KJ/kg}{437.50\ KJ/kg} = 0.84 \tag{3.10}$$

ie, one turbine stage is sufficient. Either ψ or u could be relaxed. A lower than maximum blade speed is used with ψ = 1.75.The mean pheripheral speed, u, is now obtained from equation (3.5) as:

$$U = \left[\frac{g_c \Delta_4 h_{05}}{\psi}\right]^{1/2} = \left[\frac{(1)\,367.86 \times 10^3}{1.75}\right] = 458.48\ m/s \tag{3.11}$$

In figure 3.1,

$$C_1 = \frac{C_{\theta 1}}{\sin \alpha_0} \tag{3.12}$$

Using equations (3.5) and (3.7), we get:

$$C_{\theta 1} = 1.375\,U \quad \text{and} \quad C_{\theta_2} = 0.375$$

Therefore,

$$C_1 = \frac{1.375\,U}{\sin 70^\circ} = \frac{1.375(458.48)}{\sin 70^\circ} = 670.87\ m/s \tag{3.13}$$

and,

$$C_x = \sqrt{C_1^2 - C_{\theta_1}^2} = \left[(670.87)^2 - (1.375\,U)^2\right]$$
$$= 229.46\ m/s \tag{3.14}$$

The flow coefficient is now obtained from equation (3.9) as:

$$\phi \equiv \frac{C_x}{U} = \frac{229.46}{458.48} = 0.50 \tag{3.15}$$

Determination of Inlet Flow Mach numbers

The static temperature at turbine inlet is obtained by iterating for $\bar{C}_p$, from the following equation:

$$T_{st_4} = T_{04} - \left[\frac{C_1^2}{2\bar{C}_p g_c}\right]$$
$$= 1199.82^\circ K - \left[\frac{(670.87)^2}{2(1939.2)(1)}\right] \tag{3.16}$$

or,

The speed of sound in the BOF gas at turbine inlet is given by:

$$T_{ST_4} = 1083^\circ K.$$

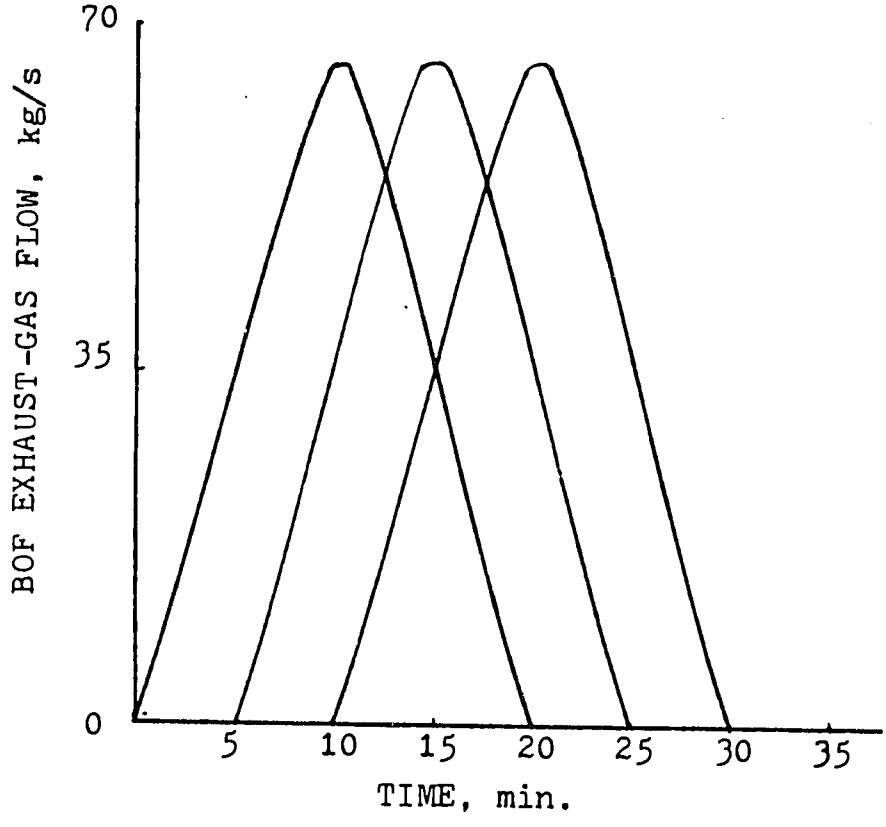

FIGURE 3.2 BOF EXHAUST-GAS FLOW FOR $t_{start\ up}$ = 5 mins.

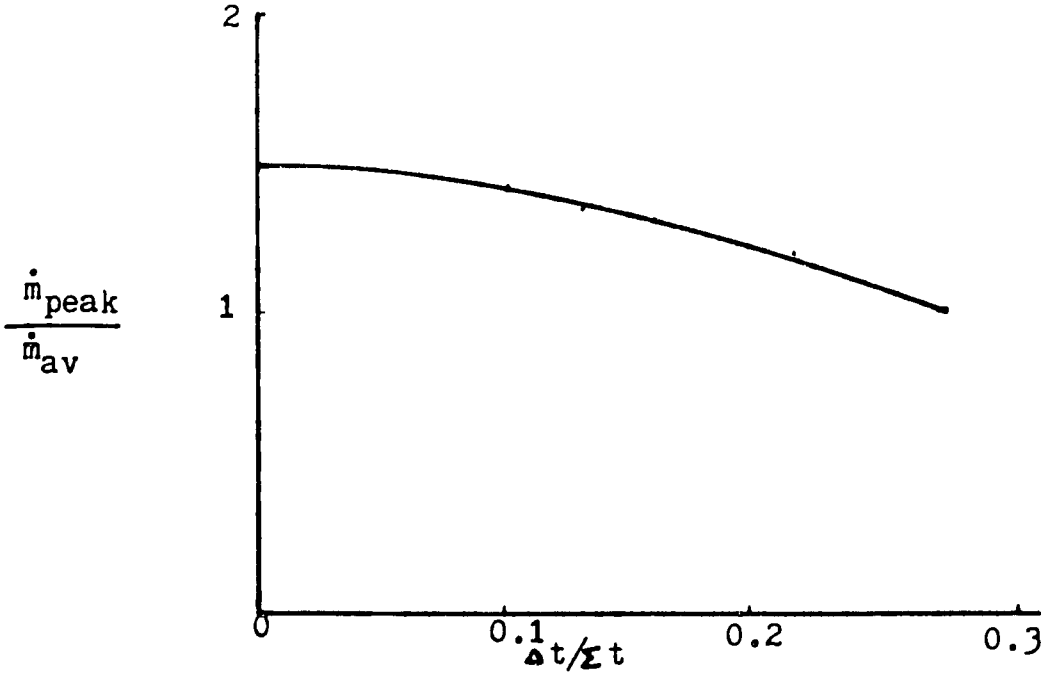

FIGURE 3.2(a) $\dot{m}_{peak}/\dot{m}_{av}$ RATIO OF BOF PEAK-EXHAUST GAS FLOW TO AVERAGE-GAS-FLOW(42.6kg/s) vs RATIO OF TIME BETWEEN BOF START-UPS TO TOTAL CYCLE TIME FOR ONE BOF(45min.)

$$a_{ST_4} = \left[\frac{g_c T_{ST4}}{\frac{1}{R} - \frac{1}{C_p}}\right] = \left[\frac{(1)\ 1083}{\frac{1}{373.69} - \frac{1}{1939.2}}\right]^{1/2} = 708.3\ m/s \tag{3.17}$$

Therefore, the absolute and relative Mach numbers at turbine rotor inlet are calculated to be:

$$M_{1ABS} = \frac{C_1}{a_{ST4}} = 0.95 \tag{3.18}$$

$$M_{1REL} = \frac{W_1}{a_{ST4}} = \frac{\left[C_x^2 + 0.375\,u\right]^{1/2}}{708.3} = 0.41 \tag{3.19}$$

Therefore a subsonic nozzle can be used.

3.3 PRELIMINARY MECHANICAL-DESIGN OF POWER-TURBINE

As discussed in chapter 2, the power turbine could be sized to handle a fraction of the peak gas flow from the furnaces. This peak mass flow of gas is a function of the chosen minimum time between BOF starts, Δt_S. If all BOFs start together, ($\Delta t_S = 0$), the peak flow would be at the highest value. As discussed in Appendix B, to avoid this high peak flow, Δt_S could be specified to be, for instance, 5 minutes. We may further reduce the required turbine size by specifying that it is to handle only a fraction of the peak flow occurring with $\Delta t_S = 5$ minutes, and the remainder of the peak flow would be diverted past the turbine to the waste-heat boiler. The turbine and alternator would then spend a larger fraction of the total time at full load, and the design power would be reduced. The final combination of by-pass and start time, Δt_S, would have to be an economic decision. One possible combination is considered next and the power turbine is sized accordingly. Suppose thirty-five percent of the peak gas flow at $\Delta t_S = 5$ minutes (figure 3.2) is bypassed, then the peak gas flow through the turbine, $\dot{m}_{TG}$, would be:

$$\dot{m}_{TG} = \left[1 - (\%\,BYPASS)\right]\left[PEAK\ GAS\ FLOW\ FROM\ FURNACES\right]$$
$$= 0.65\left[132.0\right] Kg/s = 85.8\ Kg/s \tag{3.20}$$

and for this gas flow the mass flow of steam required is obtained from equation (B.93) to be:

$$\dot{m}_{\substack{STEAM\\ REQUIRED}} = 9.40\ Kg/s$$

Therefore, the total peak flow through the turbine, $\dot{m}_{Tpeak}$, would be:

$$\dot{m}_{Tpeak} = \dot{m}_{TC} + \dot{m}_{steam\ required} = 95.20 \text{ kg/s}$$

From equation (B.103) in Appendix B, we know:

$$\dot{m}_{Tpeak} = \rho_{ST4} A_4 C_x . \tag{3.21}$$

By definition, the total and static conditions at a point are connected by an isentrope (see reference [14] chapter 7). Therefore, the static pressure at turbine inlet is given by:

$$P_{ST4} = \frac{P_{04}}{\left(\frac{T_{04}}{T_{ST4}}\right)^{\frac{c_p}{R}}} = \frac{3 \times 14.7 \text{ psia}}{\left(\frac{1199.82}{1186.00}\right)^{\frac{1941.9}{373.69}}} = 41.57 \text{ psia} \tag{3.22}$$

$$= 286.66 \ \frac{kN}{m^2}$$

The static density is then obtained from the ideal gas law to be:

$$\rho_{ST4} = \frac{P_{ST4}}{RT_{ST4}} = \frac{286.66 \ kN/m^2}{373.69 \ J/kg\,K \ 1186^\circ K} \ 1 \frac{J}{N\text{-}M} \tag{3.23}$$

$$= 0.65 \ Kg/m^3$$

Therefore with the axial velocity, C , obtained in equation (3.14), the required turbine flow area is given by:

$$A_4 = \frac{\dot{m}_{Tpeak}}{\rho_{ST4} C_x} = \frac{95.2 \ Kg/s}{0.65 \frac{Kg}{m^3} \ 229.46 \frac{m}{s}} = 0.64 \ m^2 \tag{3.24}$$

The turbine tip and hub radii are determined as follows. We first choose a hub-tip ratio. A conservative value for the inlet of a single-stage design is 0.8, (although we could use 0.6-0.9 without great compromise). The annulus area for an axial turbine is given by

$$A_4 = \pi \left[r_t^2 - r_h^2 \right] \tag{3.25}$$

or, $$0.64 = \pi \left[r_t^2 - (0.8 r_t)^2 \right]$$

and $$r_t = 0.75\,m \text{ or } 2.5\,ft,$$
$$r_h = 0.8 r_t = 0.60\,m = 2.0\,ft. \tag{3.26}$$

Therefore, the power turbine is about five feet (1.5m) in diameter with blades about six inches (0.15m) in height. The tip peripheral speed is obtained to be:

$$u_t = \frac{u}{0.9} \quad 509.42 \text{ m/s} \tag{3.27}$$

Therefore the turbine shaft speed should be:

$$\omega = \frac{u_t}{r_t} = 708 \frac{rad}{sec} \text{ or } 6{,}760 \text{ RPM}. \tag{3.28}$$

The circumference of the hub, on which the moving blades will be attached, is calculated to be 3.77m at a hub diameter of 1.2m.

For a possible spacing, s, of 0.09m (= 3.5inches), forty-two blades would be required in the turbine.

3.4 ALTERNATIVE TURBINE DESIGNS

Two other reaction turbines and an impulse turbine are considered for the energy-recovery cycle. These turbines were analyzed just as were the turbine in sections 3.2 and 3.3. The specifications and results are summarized in Table III. The velocity diagram for each of the alternative turbines is shown in figure 3.3.

3.5 CONCLUSIONS AND RECOMMENDATIONS

The fifty-percent-reaction turbine, Case T1 , is recommended for the low-pressure cycle with steam injection. As seen in table III, this turbine has the lowest inlet flow Mach numbers compared to all other designs considered. It is not as highly loaded as the other fifty-percent-reaction turbine, case T3. The impulse turbine, case T4, was considered for a possible partial-admission turbine. Since operation of several furnaces would result in fluctuating gas flow rates, each of the flow streams could be ducted through separate arcs of admission with nozzles to only a portion of the rotor

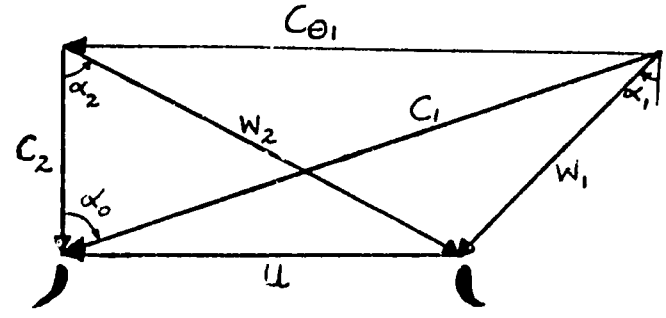

CASE T2: R_n=25%, ψ =1.5, ϕ =0.55

MEDIUM-WORK TURBINE.

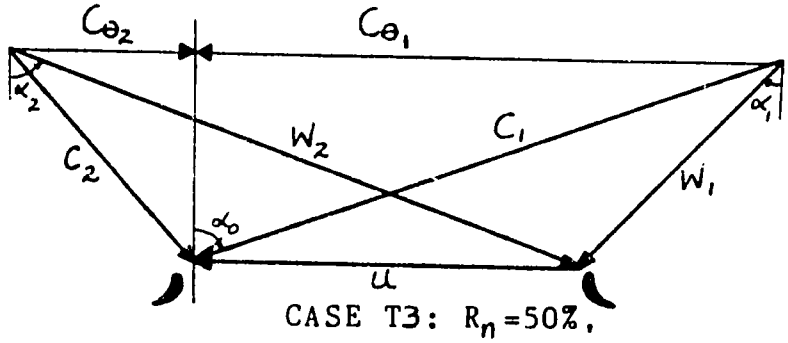

CASE T3: R_n=50%,

ψ =2.0, ϕ = 0.55

HIGH-WORK TURBINE.

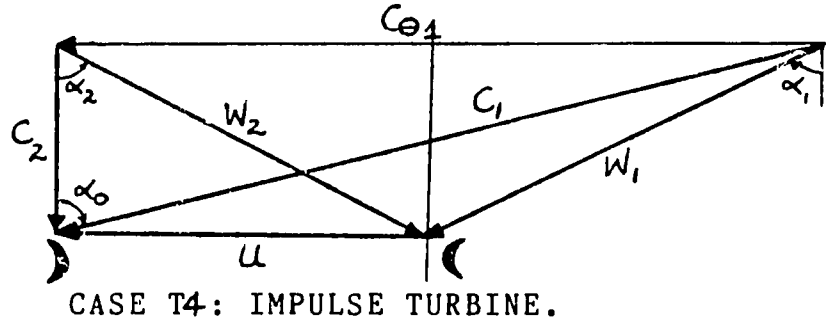

CASE T4: IMPULSE TURBINE.

HIGH-WORK TURBINE.

FIGURE 3.3 VELOCITY DIAGRAMS OF ALTERNATIVE TURBINE DESIGNS.

TABLE III

POWER TURBINE DESIGN (INCLUDING ALTERNATIVE DESIGN)

CASE	R_n (%)	ψ	ϕ	U (m/s)	C_1 (m/s)	$C_{\theta 1}$ (m/s)	$C_{\theta 2}$ (m/s)	M_1 ABS.	M_1 REL.	r_h (m)	h (m)	s (m)	n	α_1 (Deg)	α_2 (Deg)	ω (RPM)
T1	50	1.75	0.50	458.48	670.87	630.41 (=1.375u)	171.93 (=0.375u)	0.95	0.41	0.60	0.15	0.09	42	37	70	6760
T2	25	1.50	0.55	495.22	790.50	742.83 (=1.5u)	0.00 (no swirl)	1.14	0.53	0.56	0.14	0.09	39	43	62	7506
T3	50	2.00	0.55	428.87	684.60	643.31 (=1.5u)	214.44 (=0.5u)	0.97	0.45	0.60	0.15	0.09	42	43	70	6070
T4	0	2.00	0.73	428.87	912.79	857.74 (=2u)	0.00	1.35	0.78	***** SEE NOTE BELOW *****						

NOTE: The non-uniform blowing profile makes a reaction-power-turbine with variable nozzles more attractive for operation at optimum circumstances.

SPECIFICATIONS COMMON TO ALL TURBINES:

... SINGLE STAGE

... $\alpha_0 = 70°$

... $\frac{r_h}{r_t} = 0.8$

... $\dot{m}_{T_{max}} = 95.20$ kg/sec (includes steam)

blading. The entire pressure drop would thus occur in the nozzle arc and the rotor would provide a wide range of shaft power output. However, the highly non-uniform blowing profile from several BOFs would seem to require a modulating adjustment, rather than one having on-off control to each furnace exhaust. A power turbine with variable nozzles that would adjust automatically and with the exhaust from all furnaces brought into a single duct would seem to be a simpler and more effective solution. Such power turbines are increasingly being used coupled with aircraft gas turbines, for instance, and serving as naval-ship propulsion units.

A variable nozzle is recommended to precede the rotor of case T_1 . The variable geometry would warrant obtaining the required incidence angle at various mass flow rates entering the reaction turbine. A turbine exhaust diffuser could be included to handle the "swirl" and perhaps enhance turbine performance. It is recommended that the variable nozzle and the diffuser be studied further for incorporation into the power-turbine.

As seen in section 3.3, the turbine blades are about six inches (0.15m) in height at inlet, and hence large enough to incorporate internal cooling circuits. The usual coolant is compressed air, which could be tapped from the air compressor in the oxygen plant, or could be obtained from a separately driven machine. Alternatively water could be used as the blade-cooling fluid in a cycle with no steam injection and hence with a temperature, T_{04}, of 1588°K. Water-cooled blades are studied in detail in references [23] and [24] for gas-turbine cooling technology development. These, however, are still in the experimental stage.

CHAPTER 4

CONCLUSIONS AND RECOMMENDATIONS

1. The theoretical results of this thesis show that it is feasible to incorporate a steam-injected gas-turbine cycle with a pressure ratio of three into a group of basic oxygen furnaces.

2. The oxygen to be blown into the BOF during steelmaking is further compressed by a pressure ratio of three. Hence the pressure of the oxygen entering the BOF would be three times its reservoir pressure of about 150psia (1.03MPa). This increased pressure, along with the increased temperature of the oxygen due to heat exchange with the turbine exhaust, would require modification of the oxygen lance. Any "freezing" of the oxygen when it contacts the hot metal may be prevented due to the oxygen being hotter (T_{03}= 865 K) than in the conventional BOF (T_{02}= 310 K). It is recommended that the oxygen compressor be designed without any intercooling (see Appendix B).

3. The arrangements for sealing the BOF mouth before blowing would be similar to those already used in Japan and the U.S.A. for suppressed combustion. A valve that opens into the pressurized turbine-inlet manifold when the hood pressure reaches manifold pressure is required. The turbine nozzles should be adjustable to maintain approximately constant pressure. The turbine would provide surplus energy from the exhaust gases and in addition the carbon-monoxide in the exhaust could be fed to the gas mains. The lower temperatures resulting from lack of combustion could make the exhaust system potentially longer lasting. Also, for a pressure ratio of three, the exhaust duct size is reduced to one-sixteenth the area of that necessary for a conventional BOF with atmospheric combustion at the furnace mouth.

4. Steam injection is incorporated to increase power output by the turbine by added steam mass-flow (see tables I and II in chapter 2) and to decrease the turbine-inlet temperature to 1200 K, so that an uncooled long-life turbine could be specified.

5. An economic decision will have to be made to trade-off turbine size versus power and steam output by the cycle (see section 2.4 of chapter 2, and chapter 3).

6. The time between BOF start-ups, Δt_1, will have to be chosen and a control system designed accordingly for the amount of steam injected and the amount of gas flow to be bypassed past the turbine.

7. The operating parameters in the cycle permit using fairly conventional industrial components, if the existing arrangements for suppressing combustion in BOFs can be used also for pressurized units. The risks of an experimental program should therefore not be large, while the benefits seem considerable.

8. Pressurization of the BOF is recommended based on the apparently insignificant effects of pressure application on BOF steelmaking and the large amounts of power that could be produced (see section 2.1 and 2.2 of chapter 2 for details).

9. This study has proved that the proposed arrangement is feasible from the aspect of thermodynamic and mechanical design of the turbine and the overall cycle. The arrangement would involve a major change in furnace operation and exhaust treatment. Steelmakers are understandably cautious about incorporating any additions to their plant if these bring with them the potential for unreliability and consequent stoppages in steel production. The proposed arrangement could actually produce increased reliability in exhaust handling, as the gas temperatures are significantly lower and of smaller volume. But in other respects the plant would be more complex. The potential energy recovery is so large, however, that a full design study of a complete system seems warranted. A small-scale experimental trial would in any case be necessary before a full-scale conversion could be attempted.

REFERENCES

1. U.S. Steel Corporation (1971) THE MAKING, SHAPING AND TREATING OF STEEL, H.E. McGANNON, ed., 9th. edition, Herbick and Held, Pittsburgh, PA.

2. Iron and Steel Society of the American Institute of Mining, Metallurgical and Petroleum Engineers, Inc., (1982), BOF STEELMAKING VOLS I & II, INTRODUCTION, THEORY, AND DESIGN PART I & II, J.M. GAINES, ed.

3. KOBAYASHI, S, March (1981), ENERGY SAVING TECHNIQUES OF KAWASAKI STEEL, Kawasaki Steel Technical Report.

4. WILSON, D.G., V.G. FILIPENCO, M. AHDAB, M.A. McPEAK, November (1983), ENERGETICS IN THE EGYPTIAN METAL INDUSTRIES, U.S.REPORT NO.1, POTENTIAL IMPROVEMENTS IN THE SINTERING, BLAST-FURNACE AND STEEL-FURNACE PROCESSES, M.I.T Mechanical Engineering, Systems and Design Division.

5. PHILBROOK, W.O.,(1958), JOURNAL OF METALS, VOL.10, NO.7,PP477-482.

6. DICKERSON, GRAY, HAIGHT, (1974), CHEMICAL PRINCIPLES, 2nd. edition, W.A. Benjamin, Inc., Menlo Park, California 94025. 7. STONE, J.K., May (1967), THEORETICAL POSSIBILITIES OF OPERATING THE L-D PROCESS AT HIGH PRESSURES, JOURNAL OF METALS, VOL.19, NO.5, PP21-26.

8. ARLEKAR and DESMOND (1977), ENGINEERING HEAT TRANSFER, West Publishing Company, New York.

9. KRIETH, F., (1973), PRINCIPLES OF HEAT TRANSFER, 3rd. Edition, Harper & Row Publishers, New York.

10. LAIDLER, K., (1965), CHEMICAL KINETICS, 2nd. edition, PP231-238. McGraw-Hill Publications.

11. BRADLEY, R.S., and D.C. MUNRO, (1965), HIGH PRESSURE CHEMISTRY, 1st. edition, Pergamon Press, Oxford, London.

12. ROHSENOW, W.M., (1964), DEVELOPMENT IN HEAT TRANSFER, The M.I.T. Press, Cambridge, Massachusetts.

13. VAN WYLEN and SONNTAG, (1973), FUNDAMENTALS OF CLASSICAL THERMODYNAMICS, 2nd. edition, John Wiley and Sons, Inc., New York.

14. WILSON, D.G., (1984), THE DESIGN OF HIGH EFFICIENCY TURBOMACHINERY AND GAS TURBINES, The M.I.T. Press, Cambridge, Massachusetts.

15. KEENAN, CHAO, KAYE, (1945), GAS TABLES, 2nd. edition (SI units), John Wiley and Sons, Inc., New York.

16. KOLOSEUS, C., and S. SHEPARD (1985), THE CHENG CYCLE OFFERS FLEXIBLE COGENERATION OPTIONS, Modern Power Systems, March 1985, PP39-43.

17. EL MAGHRABY, M.G., and D.G. WILSON, Nov. (1982), ENERGETICS IN THE EGYPTIAN METAL INDUSTRIES, Report No.1, Analysis of the Present Status in the Iron and Steel Complex, Helwan.

18. WHEELER, D.H., FUME CONTROL IN L.D. PLANTS, Journal of Air Pollution Control Association, 18, (2) Feb. (1968), PP98-101.

19. SPIERS, H.M., Editor, TECHNICAL DATA ON FUEL, 5th. edition, The British National Committee, World Power Conference, 201 Grand Buildings, London (1955).

20. MAUDLIN, J., (1979), REPUBLIC CLEVELAND'S BOF SUPPRESSED COMBUSTION SYSTEM, Iron and Steel Engineer, Sept. 1979, PP25-32.

21. REAY, D.A., (1979), HEAT RECOVERY SYSTEMS, A Directory of Equipment and Techniques, published by E and F Spon Ltd., London. PP17-24.

22. SPAULDING, D.B., J. TABOREK , (1983), HEAT EXCHANGER DESIGN HANDBOOKS, VOL. 1 To 5. Hemisphere Publishing Corp., N.Y., U.S.A..

23. HIRSCHKRON, R., R.F. MANNING, J.F. HAYNES, (1981), TURBINE COOLING SYSTEM WATER INJECTION, G.E.-NASA Technical Project, NAS3-21579, GE, AEBG, Lynn, MA.

24. COHN, A., W.H. DAY, M.W. HORNER, of General Electric Co., Schenectady, N.Y., (1979), WATER-COOLED GAS TURBINE TECHNOLOGY DEVELOPMENT: FUELS FLEXIBILITY, ASME paper 79-GT-72.

25. CORSO, J.D., and C.T. HANSOTTE, (1980), EFFECTS OF VARYING HOT METAL ANALYSIS AND TEMPERATURES ON BOF OPERATIONS, Inland Steel Co., East Chicago, IN., March 1980, presented at the 63rd. National Open Hearth and Basic Oxygen Steelmaking Conference.

APPENDIX A

A.1 PHYSICAL CHEMISTRY OF OXYGEN STEELMAKING

The physical chemistry of steelmaking is an extensive subject and this appendix discusses only the basic concepts of the subject that directly pertain to the pressurized BOF steelmaking process. First, the steelmaking reactions and the effects of pressure and temperature on these reactions are discussed. Next, the effect of temperature on solubility of two important elements in iron is briefly studied.

Definitions

Solutions

A solution is defined in reference [2] as a homogeneous gas, liquid or solid mixtures any portion of which has the same state properties. In metallic, liquid and solid solutions of iron-base alloys encountered in steelmaking, the concentrations of constituent elements is usually reported in mass percent. When considering the thermodynamic properties of such solutions the concentrations are converted to atomic concentrations. The atom fraction, N_i , is given by the ratio:

$$N_i \equiv \frac{n_i}{\Sigma n} \qquad (....A.1)$$

here n is the number of gram atoms of element i per unit mass of the substance and n is the total number of atoms. Since the composition is usually given in mass percent, n_i per 100 grams of the substance is:

$$n_i = \frac{\%\ \text{mass of element } i\ (\text{per } 100g \text{ of substance})}{M_i} \qquad (....A.2)$$

where M_i is the atomic mass.

Activity

The activity a_i of the ith component in the solution, is defined in reference [2] as:

$$a_i \equiv \frac{p_i}{p_i^o} \qquad (....A.3)$$

where p is the partial pressure of the ith component in the gas phase and p is the partial pressure of the pure ith component in a reference state (usually the standard state).

Equilibrium Constant

Suppose the following equlibrium equation occurs at constant temperature and pressure:

$$xX + yY + \ldots \rightleftarrows uU + vV + \ldots \qquad (\ldots.A.4)$$

where x, y, u, v,... are the number of moles of the chemical compounds X, Y, U, V,...respectively. Then in terms of activities of reactants and products, the equilibrium constant, K_{eq} is defined in reference [2] as:

$$K_{eq} \equiv \frac{(a_U)^u (a_V)^v \ldots}{(a_X)^x (a_Y)^y} \qquad (\ldots.A.5)$$

From the definition of activity, equation (A.3), in reactions involving gases and vapors, the equilibrium constant is given in terms of the partial pressures of the reacting gases. Therefore, if X, Y, U, V are gases:

$$K \equiv \frac{(P_U)^u (P_V)^v \ldots}{(P_X)^x (P_Y)^y \ldots} \qquad (\ldots.A.6)$$

Steelmaking Reactions and the effects of Pressure and Temperature on the Equilibrium Constant

The reactions occuring in the steelmaking processes are essentially oxidation reactions. The hot metal produced by the blast-furnace contains a number of impurities like silicon, sulphur, phosphorous, manganese, which along with carbon are removed by oxidation during the BOF operation. The equlibrium changes accompanying these reactions at elevated temperatures and pressures are evaluated in this section.

Equilibrium represents a balance between two opposing reactions. How sensitive is this balance to the changes in the conditions of a reaction ? What can be done to change the equilibrium state ? These are practical questions when the yield of CO in BOF exhaust gases is to be increased to obtain energy benefits due to its calorific value. A closed, pressurized BOF is proposed to prevent combustion of CO and to increase availability of the exhaust gases. The primary effect of increasing pressure and the effect of consequent increase in temperature, on equlibrium of BOF steelmaking reactions are discussed next.

The well known Le Chatelier's principle discussed in reference [6] and [7] may be stated as follows:@quotation("If a system in equilibrium is subjected to an influence which upsets the equlibrium, the change will take place in such a direction so as to oppose the influence and will tend to restore equilibrium.")

The equilibriumconstant, K_{eq} , is not altered by a pressure change at constant temperature. However, the relative amounts of reactants and products will change in a way that can be predicted from Le Chatelier's principle. In the stoichiometric reaction of carbon-monoxide with oxygen, three moles of reactants become two moles of products:

$$2CO(g) + O_2(g) \rightleftarrows 2CO_2(g)$$

(....A.7)

According to Le Chatelier's principle, pressurization of the system will promote CO formation because the total number of moles of gas produced is decreased to oppose the influence of pressure increase.

The yields of required products can be enhanced by increasing the equilibrium constant so that the ratio of products to reactants at equilibrium is larger. The equilibrium constant is usually temperature-dependant. In general, both forward and reverse reactions are speeded up by increasing temperature, because the molecules move faster and collide more often. But due to Le Chatelier's principle, if the forward half of an equilibrium reaction is exothermic, then K_{eq} will decrease as the temperature increases; if it is endothermic, K_{eq} will increase. Reaction (A.7) is exothermic and the decrease of K_{eq} can be verified as follows. From reference [6], the equilibrium constant is defined as:

$$K_{eq} \equiv e^{-(\Delta G_T^o/RT)}$$

(....A.8)

where ΔG_T^o is the free energy of reaction at a specified temperature T (°K), and R is the universal gas constant. At the standard temperature of 298° K, the free energy of the reaction is obtained from reference [6] as:

$$\Delta G_{298}^o = \{2(-94.26-(0.0)-2(-32.81)\}\ kcal$$
$$= -122.90\ kcal$$

(....A.9)

Therefore from equation (A.8), with R=1.99 x 10 kcal/ K, the equilibrium constant is calculated to be:

$$K_{eq} = 1.01 \times 10^{90}$$

(....A.10)

when the temperature is raised, the absolute value of free energy at the higher temperature is less than the absolute value of the free energy at 298° K (reference [6]), and hence K_{eq} at the higher temperature is less than that at 298° K. So, K_{eq} decreases with increasing temperature. From reference [1], K_{eq} for reaction (A.7) is also given as a function of temperature to be:

$$\text{Log}\ K_{eq} = \frac{29508}{T} - 9.054$$

(....A.11)

and from this equation it can be checked that K_{eg} decreases with increasing temperature. Such exothermic reactions that form CO_2 tend to be suppressed be any rise in temperature. Therefore, as desired, dissociation of CO_2 to CO is enhanced.

In the exothermic reaction of carbon in molten-iron and oxygen, one mole of reactant gas forms two moles of the product gas:

$$2C\ (\text{in molten metal}) + O_2 \rightleftarrows 2CO(g)$$

(....A.12)

and as expalained before, pressurization favors dissociation of carbon-monoxide. The equilibrium constant for reaction (A.12) is given by:

$$K_{eg} = \frac{(P_{CO})^2}{(a_C^2 P_{O_2})}$$

(....A.13)

Assuming at constant temperature K_{eg} and the carbon content are unchanged, the partial pressure of oxygen would increase with increasing partial pressure of CO. The oxygen potential, defined in reference [2] as:

$$\text{Oxygen Potential} \equiv RT \ln P_{O_2}$$

(....A.14)

could become high enough to oxidize the iron and hence oxygen blowing would have to be controlled to prevent excessive oxidation of iron.

The oxidation of silicon to silica ia an exothermic reaction (reference [2]) and provides some of the heat necessary to raise the temperature of the bath during oxygen blowing. In this reaction, two moles of reactants become one mole of product:

$$Si(l) + O_2(g) \rightleftarrows SiO_2(g)$$

(....A.15)

and hence the removal of an impurity, silicon, is promoted by increasing pressure. Similarly in the reaction,

$$2Mn(l) + O_2(g) \rightleftarrows 2MnO(s)$$

(....A.16)

removal of manganese from molten-iron is promoted by pressurizing the BOF. Removal of phosphorous from iron can be achieved only by oxidation during steelmaking under a basic slag. The phosphorous-oxygen reaction can be represented as (reference [2]):

$$2P(\text{in metal}) + 5O(\text{in metal}) \rightleftarrows P_2O_5\ (\text{dissolved in slag})$$

(....A.17)

The temperature dependence of the equilibrium constant for the above reaction is obtained from reference [2] as:

$$\log K_{eq} = \frac{36850}{T} - 29.07 \qquad (....A.18)$$

It is seen in equation (A.18) that low temperature favors better dephosphorization but a high temperature is required to dissolve sufficient lime in the slag, essential for phosphorous removal.

Most reactions in the BOF are exothermic. As discussed before, these would be somewhat suppressed by an increase in temperature in the BOF. Therefore, it is suggested that the scrap charge be increased to absorb the heat liberated. Reference [2] states that the most feasible way to date of controlling steelmaking in the BOF is by controlling the composition of the hot metal and scrap, and adjusting the oxygen blow for the desired endpoint carbon based on past experience. It is recommended this method of controlling and adjusting be performed for the suggested pressurized system.

Solubility of Carbon and Oxygen in Iron

The effect of increasing temperature on carbon content of iron is briefly discussed in the following. The iron-carbon phase equilibrium diagram, figure A.1, is at a total pressure of one atmosphere. From reference [1] it is obtained that with sufficient time, iron-carbon alloys containing austenitic and cementite decompose to austenite and graphite. The solubility of graphite (carbon) in liquid iron is given in reference [2] as:

$$[\%C] = 1.30 + 2.57 \times 10^{-3} t\,(^\circ C)$$

(....A.19)

Thus increasing temperature in the system increases [% C] in the liquid iron and this could require increasing oxygen-blow time to obtain end-point carbon.

The solubility of oxygen in molten-iron in equilibrium with pure iron-oxide was determined by Chipman et al (reference [1]) and the variation of solubility with temperature is represented by the following equation:

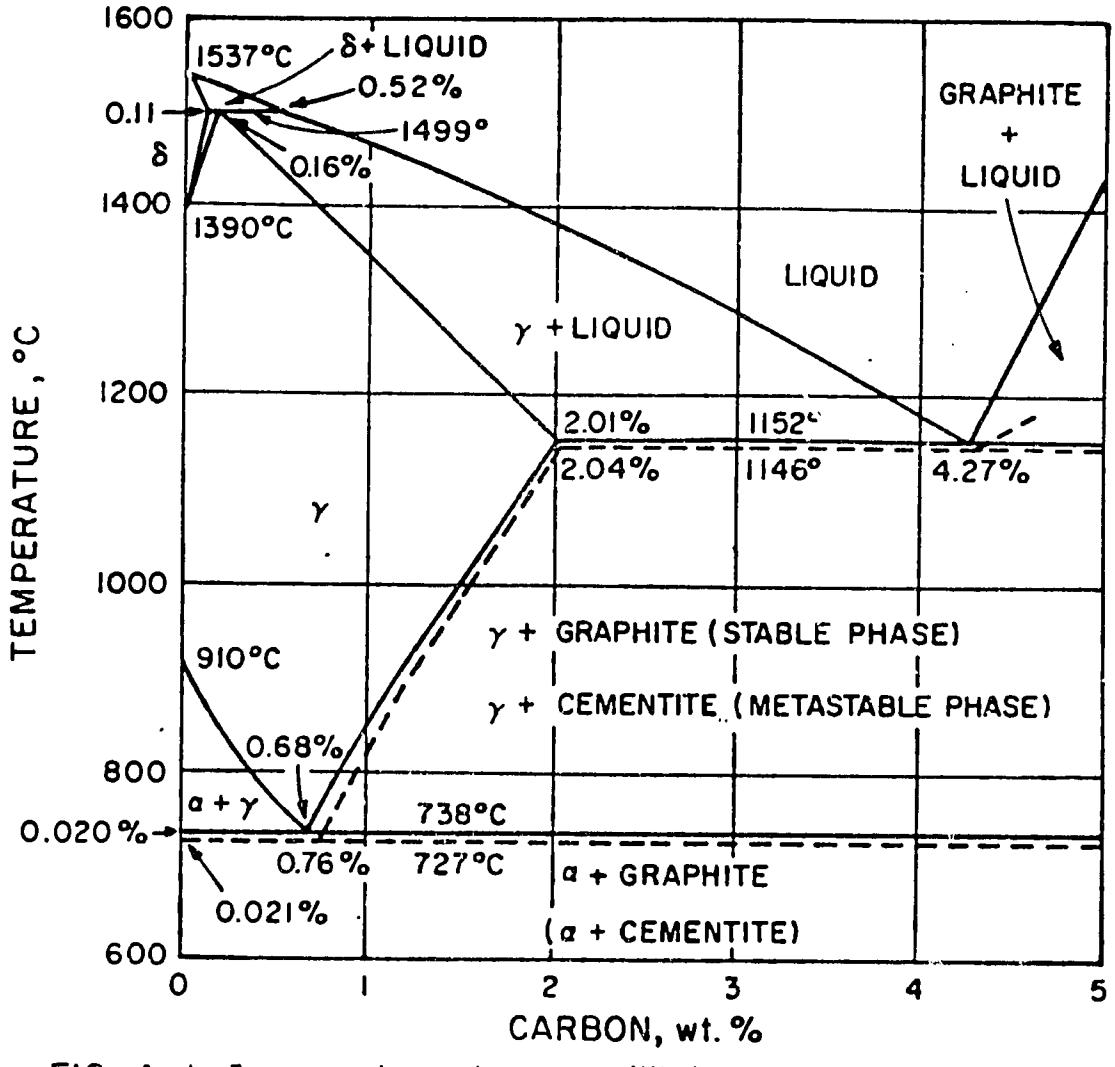

FIG. A-1 Iron-carbon phase equilibrium diagram. Dashed line represents phase boundary for metastable equilibrium with cementite.

$$\log [\% O] = \frac{-6320}{T} + 2.734 \qquad (....A.20)$$

From equation (A.20), an increase in temperature in the BOF could increase the solubility of oxygen in iron, at equilibrium. If this oxygen remains in the steel, it could combine with the carbon in the steel to form carbon monoxide resulting in blowholes forming during solidification of ingots and castings. As discussed in reference [2], if the concentrations of silicon and manganese or other deoxidizers are sufficiently high, the oxygen in solution in steel will be maintained at low levels during solidification, such that the carbon-oxygen reaction will not take place and formation of blowholes will be prevented.

A.2 THEORY OF BOF REACTION RATES

One of the major advantages of the BOF process is its speed of refining. It is also this high rate of chemical reactions that causes problems in attempting to control the operation. During the steelmaking process heat that is evolved or absorbed due to the chemical reactions, the mass transfer that is involved between several phases, the nucleation of bubbles and perhaps emulsions and foams within the bath make BOF steelmaking a complex process.

Chemical Reaction Rates

Reference [1] defines the rate of a reaction as the time derivative of concentration dC/dT, i.e. change in concentration of the reacting species with time of reaction, and this is proportional to the product of the concentrations of the reactants. In the reaction below:

$$A + B \rightarrow AB \qquad (....A.21)$$

when the concentration of B is very high and B may thus be assumed to be in infinite supply, then the rate of reaction is dependant only on the concentration of A. The rate of decrease of concentration of A is proportional to the concentration C_A of A or:

$$-\frac{dC_A}{dt} = KC_A \qquad (....A.22)$$

where k is the specific reaction-rate constant. Equation (A.22) can be rearranged as follows:

$$\frac{dC_A}{C_A} = -K dt$$

(....A.23)

and integrated to obtain:

$$C_A = C_A^{\circ} e^{-Kt}$$

(....A.24)

where C_A° is the initial concentration.

Rate constants, as in equation (A.24) are empirical and must be determined by trial and error fitting of experimental data (reference [2], chapter 5). The absolute reaction-rate theory enables the prediction of rate constants from principles rather than experiments. Based on the absolute reaction-rate theory, reference [1] gives the rate constant in terms of other factors:

$$K = \frac{RT}{Nh} \quad \frac{\gamma_{C_A} \gamma_{C_B}}{\gamma_{C^*}} \left(e^{\Delta S^*/R}\right)\left(e^{-\Delta H^*/RT}\right)$$

(....A.25)

where,

$R \equiv$ gas constant;

$T \equiv$ absolute temperature;

$N \equiv$ Avogandro's number;

$h \equiv$ Planck's constant;

$\gamma \equiv$ activity co-efficient;

C_A and $C_B \equiv$ concentration of reactants A and B respectively;

$C^* \equiv$ concentration of activated complex;

$\Delta S^* \equiv$ entropy change of the activated complex;

$\Delta H^* \equiv$ enthalpy change of the activated complex.

Assuming that the activity coefficients do not change much in the composition range being considered and as discussed in reference [1] B, section B.1, ΔH^* and ΔS^* can be assumed to be independent of temperature, the first term in equation (A.25) can be assumed to remain constant. Thus with:

$$A = \frac{RT_m}{Nh} \quad \frac{\gamma_{C_A} \gamma_{C_B}}{\gamma_{C^*}} e^{(\Delta S^*/R)}$$

(....A.26)

where T is a mean temperature, the specific reaction-rate constant in equation (A.25) can be expressed as:

$$K = Ae^{-\Delta H^*/RT}$$

(....A.27)

Influence of Temperature on Reaction Rates

In general, equation (A.27) describes the variation of the rate constant with temperature. At the temperatures involved in BOF steelmaking, it is believed (reference [2] chapter 5) that the chemical reactions themselves do not limit the rate of reaction. At elevated temperatures, the kinetics of the reactions can be studied by dividing the rate-controlling processes into two major classes:

1) transport processes, and

2) chemical processes.

Transport Processes

In the BOF, the metallurgical reactions occur in the slag, metal and gas phases. For a reaction to occur between phases, the reactants and products must be transported to and from the interfaces. In oxidation reactions between solid metal and gases, it is found, (reference [1]), that the rate of reaction, dx/dt, is inversely proportional to the thickness x of the reacted layer at the interface, i.e.,

$$\frac{dx}{dt} = \frac{k}{x}$$

(....A.28)

By rearranging and integrating equation (A.28) the following relation is obtained:

$$x^2 \propto 2kt$$

(....A.29)

This is known as the parabolic law and can also be derived from the solution of Fick's law for unidirectional diffusion (reference [1], chapter 13). For example, the rate of reaction

$$Fe + \tfrac{1}{2}O_2 \rightarrow FeO$$

(....A.30)

is given in reference [1] by the following parabolic expression:

$$\frac{W}{A} = k\sqrt{t} \qquad (....A.31)$$

where,
W/A is the weight increase per unit surface area;

k is the rate constant; and

t is the time of oxidation.

Since reaction A.30 is in accordance with the parabolic law, the rate-controlling process is diffusion. At a given time, the rate of oxidation increases at higher temperatures as seen in figure A.2.

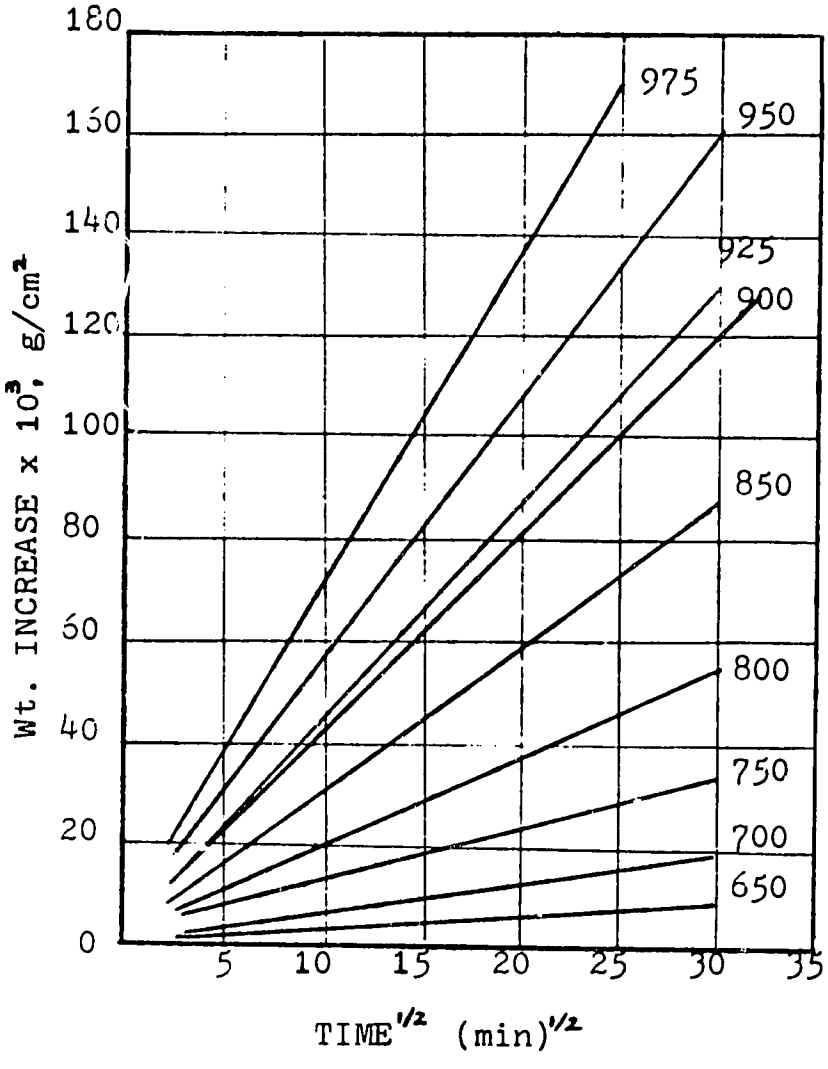

FIGURE A.2 PARABOLIC PLOT FOR THE OXIDATION OF IRON IN OXYGEN AT 1.0atm. FOR TEMPERATURES WITHIN THE RANGE 650° - 975°C (reference [1])

Chemical Processes

One of the reaction steps in gas-solid systems is the adsorption of gaseous reactants and products from the surface of the solid phase. As discussed in reference [1], chapter 13, there are two types of adsorptions:

1. Absorption that is brought about by forces of a physical nature, known as van der Waal's adsorption and accompanied by a small heat change of about 5 kcal per mole or less.

2. If the adsorbed gas interacts strongly with the solid substance, this is called chemisorption, which is accompanied by heat evolution, as in an exothermic reaction, of 20 kcal per mole or more. Usually van der Waal's adsorption occurs at lower temperatures but chemisorption predominates with increasing temperature. So the increase in temperature in the pressurized BOF could provide additional energy due to chemisorption.

In general, as seen in equation A.27, increasing temperature could cause a significant increase in the rate of reactions. In reference [10], for reactions in solutions, a rough generalization is made that the reaction rate is doubled by a rise in temperature of 10° C.

Influence of Pressure on Reaction Rates

For reactions such as the one in equation A.21, the relationship connecting the equilibrium constant, the volume and the pressure at constant temperature is obtained from reference [10] as:

$$\left(\frac{\partial \ln K_{eq}}{\partial P}\right)_T = -\frac{\Delta V}{RT} \qquad (....A.32)$$

Since the rate constant is proportional to the equilibrium constant,

$$K = \frac{RT}{Nh} K_{eq} \qquad (....A.33)$$

equation A.32 can also be written as:

$$\left(\frac{\partial \ln K}{\partial P}\right)_T = -\frac{\Delta V}{RT} \qquad (....A.34)$$

According to this equation, the rate constant of a reaction increases with increasing pressure if ΔV is negative, i.e. if the final (product) state has a smaller volume than the initial state. If ΔV is positive, the reaction-rate constant decreases with increasing pressure. As seen in equation (A.7) and (A.12), ΔV is negative and positive respectively. This would suggest an increase in the rate of reactions for CO formation in the pressurized BOF and a decrease in k for CO_2 formations. However,

as shown in reference [10], significant changes in reaction rates occur only at high pressures, in the order of 60 atmospheres and so at pressures in the order of 3 atmospheres the change in rate could be negligible.

Nucleation

The nucleation of bubbles within the BOF bath is essential for refining to occur. Reference [12] presents the following relationship between pressure, surface tension and radius of curvature of a spherical bubble of vapor in a pure liquid:

$$P_v - P_L = \frac{2\sigma}{r} \qquad (....A.35)$$

Using the Clausius-Clapyron equation and the perfect-gas law the vapor pressure can be expressed as follows:

$$\frac{dP_v}{dT_v} \cong \frac{h_{fg}}{T_v} \cong \frac{h_{fg} P_v}{R_v T_v^2} \qquad (....A.36)$$

Integrating equation A.36 and combining with with equation A.35, we get:

$$\ln P_v \Big|_{P_v}^{P_L} \cong \frac{-h_{fg}}{R_v T_v} \Big|_{T_v}^{T_{sat}}$$

$$T_v - T_{sat} = \frac{R_v T_{sat} T_v}{h_{fg}} \ln\left(1 + \frac{2\sigma}{P_L r}\right) \qquad (....A.37)$$

Pressurization of the BOF will result in an increase in pressure P_L of the liquid (molten-iron) and an increase in saturation temperature of the liquid. This in turn, as seen in equation (A.37), decreases the surface tension, σ, at the liquid-vapor interface. The decreasing surface tension with increasing pressure could result in lowering the superheat, ($T_v - T_{sat}$), required for nucleation to initiate.

A.3 SCRAP MELTING

With the fluctuation in availability of hot metal from the blast-furnace and the need to recycle steel, steel-scrap addition during BOF steelmaking has become an important topic. Several references report that scrap accounts for about 30 percent by mass of the total charge to the BOF. Reference [2] chapter 13, pp879-881, provides a detailed calculation of charge per metric ton of steel. The calculations are simplified and are summarized below.

From the known compositions and temperatures of the materials to be charged, and the target temperature and compositions of the steel, the masses of hot metal and steel scarp are determined by a mass-energy balance.

The mass balance equation is given as:

$$\Sigma (W_i \times S_i) = 1.0 \text{ Metric Tons Steel} \qquad (....A.38)$$

and the energy balance equation is:

$$\Sigma (W_i \times Q_i) + Q_{LOSS} = 0 \qquad (....A.39)$$

where,

W_i = metric tons of material i per metric ton steel;

S_i = mass of steel per metric ton material i. This is a known quantity;

Q_i = heat evolved or absorbed when one metric ton of material is converted; also a known quantity.

Q_{LOSS} = heat losses per metric ton steel made; a known quantity.

Therefore, to determine the masses of hot metal (HM) and steel scrap (SS), equations (A.38) and (A.39) can be written as:

$$W_{HM} \times S_{HM} + W_{SS} \times S_{SS} + \underbrace{(\Sigma W_i S_i)}_{\text{Known quantities of other additions}} = 1.0 \text{ M. Ton Steel} \qquad (....A.40)$$

$$W_{HM} + Q_{HM} + W_{SS} \times Q_{SS} + \underbrace{(\Sigma W_i Q_i)}_{\text{Known quantities of other additions}} + Q_{LOSS} = 0 \qquad (....A.41)$$

The two unknown quantities W and W are then determined by solving equations (A.40) and (A.41) simultaneously. In reference [2] the following masses are obtained:

W_{HM} = 0.776 Metric Tons

W_{SS} = 0.289 Metric Tons

(....A.42)

Thus scrap forms about 29% by mass of the total charge by a mass-energy balance. As explained in section (A.1) of this appendix, pressurization could result in some heat liberation within the BOF. Suppose this Q_{LIB} is included in equation (A.41); then for the same values of Q_{HM}, Q_{SS}, $(\Sigma_{KQOA} W_i Q_i)$ and Q_{LOSS} as before, simultaneous solution of equations (A.40)

and (A.41) will show W_{SS} to increase and W_{HM} to decrease from the values in equation (A.42). Hence more scrap could be added as suggested in reference [7].

An important conclusion is made in reference [2] on scrap melting. Based on experiments, it is concluded that the most important factor in rapid melting of scrap is its thickness. heavy bundle of thin sheet will quite rapidly; whereas a thick slab of the same mass will take much longer to melt.")Also, the size of the scrap that may be used is limited by the duration of the oxygen blow, as shown in figure A.3.

A.4 SURFACE PHENOMENA OF LIQUID METALS AND SLAGS

The total rate of heat and mass transfer are defined in references [8] and [9] as follows. In heat transfer, the total heat transferred per unit time, U, is defined as:

$$U = hA\Delta T = qA \qquad (....A.43)$$

where,

h is the heat-transfer coefficient;

A is the total area of heat transfer;

ΔT is the characteristic temperature difference; and

q is the heat flux per unit area.

In mass transfer, the total amount of a component transferred per unit time is:

$$J = j_i A \qquad (....A.44)$$

where,

j_i is the molar flux of component i; and

A is the interphase area.

From equations (A.43) and (A.44), it can be seen that larger the area, the more rapidly the reactions proceed. But areas of the order of vessel dimensions are not sufficient to account for the very high observed rates of reaction in the BOF. Current theories rely heavily on the formation of a slag-metal-gas emulsion to account for the required large reaction surface. the phenomena of emulsions and foams are discussed briefly in this appendix and a detailed discussion on emulsions and foams in BOF steelmaking can be found in reference [2], chapter 5.

Reference [2] defines emulsions as systems consisting of small droplets or gas bubbles imbedded in a liquid medium and the distances separating the neighbouring droplets or bubbles are large enough to allow the independent movement of the drops or bubbles. When the volume of the movement of the liquid medium in an emulsion is small when compared with the total volume of the

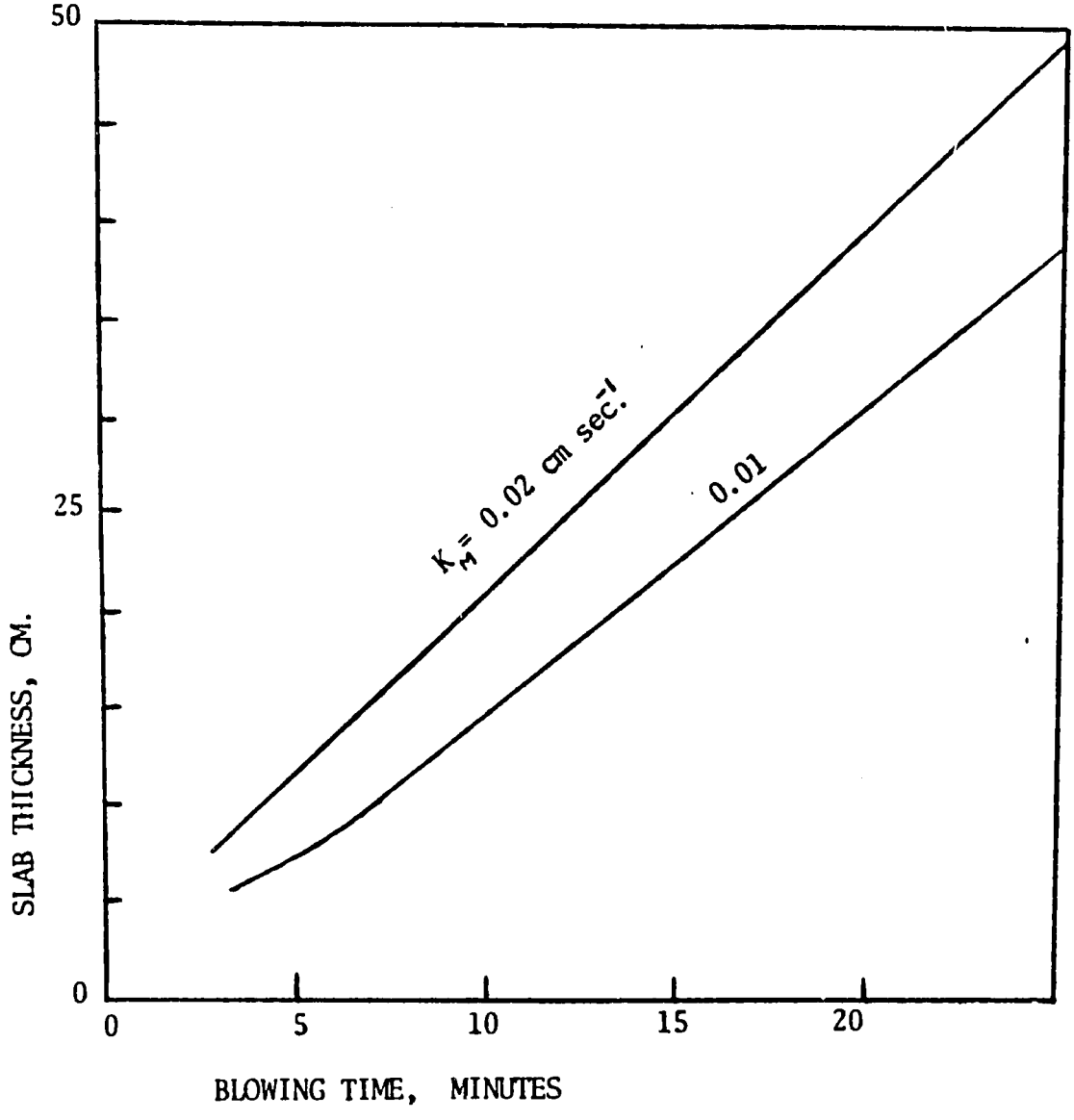

FIGURE A.3 CALCULATED MAXIMUM THICKNESS OF SLABS THAT WILL IN A GIVEN BLOWING TIME AND INDICATED ASSUMED MASS TRANSFER COEFFICIENTS; REFERENCE [2]

gas bubbles, the medium will be present only in the form of their films separating the adjacent bubbles; these cannot move freely, and the whole system is then called foam. The most important feature of any emulsion or foam is the large increase of the interfacial area between two phases.

Since the surface (interfacial) tension, γ , is the work necessary for the formation of 1 cm of new surface, the energy requirement for emulsifying a liquid or a gas in another liquid will increase with increasing γ. When the specific interface decreases, energy will be liberated. The destruction of an emulsion is a spontaneous process, since any decrease of the specific interface is accompanied by a corresponding decrease of the total surface energy. Therefore, a low interfacial tension favors both formation (since less energy is required) and retention (slower decrease of total surface energy) of an emulsion. In the BOF, the slag/gas interface is of most concern since the formation and stability of gas emulsions and slag foams directly depend on the structure and properties of the interface. As shown in reference [2] in the slag/gas interface, the surface tension decreases with increasing temperature. So in the pressurized BOF the increase in temperature could favor emulsion and the resulting increase in interfacial area could enhance the rapid rates of reaction during steelmaking.

APPENDIX B

B.1 THERMODYNAMICS OF GAS TURBINE POWER CYCLES

This appendix presents the theory in thermodynamics used to determine results in the chapter on energy recovery from pressurized BOF exhaust gases.

The First Law of Thermodynamics for a Flow Process

The expression of the first law of thermodynamics for a steady-state, steady-flow (SSSF) process is given as follows:

$$\dot{Q}_{cv} + \sum \dot{m}_i \left(h_i + \frac{V_i^2}{2g_c} + Z_i \frac{g}{g_c} \right) = \sum \dot{m}_e \left(h_e + \frac{V_e^2}{2g_c} + Z_e \frac{g}{g_c} \right) + \dot{W}_{cv} \qquad (....B.1)$$

In words, the law states that the rate of heat transfer into a control volume plus rate of energy flowing in as a result of mass transfer is equal to the rate of energy flowing out as a result of mass transfer plus the power output which in our case is associated with shaft work.

The continuity equation of mass flowrates for a SSSF process is given as follows:

$$\sum \dot{m}_i = \sum \dot{m}_e \qquad (....B.2)$$

When only one flow stream enters and one leaves the control volume, the equation (B.2) becomes:

$$\dot{m}_i = \dot{m}_e = \dot{m} \qquad (....B.3)$$

and equation (B.1) can be written as:

$$\dot{Q}_{cv} + \dot{m} \left(h_i + \frac{V_i^2}{2g_c} + Z_i \frac{g}{g_c} \right) = \dot{m} \left(h_e + \frac{V_e^2}{2g_c} + Z_e \frac{g}{g_c} \right) + \dot{W}_{cv} \qquad (....B.4)$$

Assuming the changes in kinetic and potential energies are negligible and rearranging equation (B.4), we have:

$$q + h_i = h_e + w \qquad (....B.5)$$

where, by definition,

$$q \equiv \frac{\dot{Q}_{cv}}{\dot{m}} \quad \text{and} \quad w \equiv \frac{\dot{W}_{cv}}{\dot{m}} \qquad (....B.6)$$

For an adiabatic, SSSF process, equation (B.5) becomes:

$$W = h_i - h_e \qquad (....B.7)$$

The constant-pressure specific heat, C , is defined by the relation:

$$C_p \equiv \left(\frac{\partial h}{\partial T}\right)_p \qquad (....B.8)$$

Since the enthalpy of a perfect gas is a function of temperature only (see reference [13]), and is independent of pressure, it follows that:

$$C_p = \frac{dh}{dT} \qquad (....B.9)$$

or,

$$dh = C_p dT \qquad (....B.10)$$

Thus, with equation (B.10), equation (B.7) becomes:

$$W = C_p (T_i - T_e) \qquad (....B.11)$$

For a perfect gas, as opposed to an ideal gas, C is a function of temperature and in our calculations C for carbon monoxide, oxygen and carbon dioxide is determined at an average temperature, where:

$$T_{av} \equiv \frac{T_i + T_e}{2} \qquad (....B.12)$$

<u>Thermodynamic Functions for Analysis Of Major Components In the Power Cycle</u>

<u>Compressors and Turbines</u>

Assuming a SSSF process, equation (B.11) can be applied for adiabatic compressors and turbines with a perfect gas the working fluid. Equation (B.11) in terms of total temperatures, a specific heat at an average of these temperatures, and the work output can be alternatively expressed as follows:

$$i W_e = i \bar{C}_{pe} (T_{oi} - T_{oe}) \qquad (....B.13)$$

Since the temperature of the fluid is increased due to the increase in pressure during compression, T_{0i} is greater than T_{0e} and hence the work is negative. A turbine decreases the pressure of the working fluid resulting in a temperature drop and hence the work is positive. Negative work means work is done on the fluid and positive work means work is done by the fluid. Hence, we speak in terms of work or power output by the turbine and work or power required to run the compressor. The difference between the power output and the power required by a cycle gives the net power available from the cycle for useful purposes (like generating electricity).

When a gas undergoes a reversible process in which there is heat transfer, the process frequently takes place in such a manner that a plot of log P vs log V is a straight line (see reference [13], chapter 7). This process is called a polytropic process and the relationship between gas pressure and volume is given by:

$$PV^n = \text{constant} \qquad (....B.14)$$

where, for an isentropic process,

$$n = \gamma \qquad (....B.15)$$

Thus, as shown in reference [13],

$$P_1 V_1^{\gamma} = P_2 V_2^{\gamma} \qquad (....B.16)$$

From the perfect gas law, we know that:

$$V = \frac{mRT}{P} \qquad (....B.17)$$

Substituting equation B.17 into equation B.16, the following relation is obtained:

$$P_1\left(\frac{mRT_1}{P_1}\right)^{\gamma} = P_2\left(\frac{mRT_2}{P_2}\right)^{\gamma} \text{ or, } \frac{T_2}{T_1} = \left(\frac{P_2}{P_1}\right)^{\frac{\gamma-1}{\gamma}} \qquad (....B.18)$$

By definition,

$$\gamma \equiv \frac{C_P}{C_v} \qquad (....B.19)$$

and with,

$$C_p = C_v + R \qquad (....B.20)$$

the following useful relation is derived:

$$\frac{\gamma - 1}{\gamma} = \frac{R}{C_p} \qquad (....B.21)$$

Therefore, equation (B.18) can be expressed as:

$$\frac{T_2}{T_1} = \left(\frac{P_2}{P_1}\right)^{\frac{R}{C_p}} \qquad (....B.22)$$

Efficiency of Turbomachinery

The efficiency of a turbomachine is defined as a comparison between the actual performance of the machine under given conditions and the performance that would have been achieved in an ideal process. Therefore, if we denote the actual work done per unit mass of gas flow through the turbine as W_{ae} and the work that would have been done in an ideal process that is reversible, adiabatic or isentropic process between the inlet state and the turbine exhaust pressure as W_{se} , the efficiency of the turbine is defined as:

$$\eta_{se} \equiv \frac{w_{ae}}{w_{se}} \qquad (....B.23)$$

The efficiency of a compressor is the inverse of this ratio, or

$$\eta_{sc} \equiv \frac{w_{sc}}{w_{ac}} \qquad (....B.24)$$

The isentropic efficiency defined in equations (B.23) and (B.24) has serious disadvantage in that its value is a function of pressure ratio as well as of losses, as discussed in reference [14], chapter 2. To avoid this influence of pressure ratio on isentropic efficiency, the limiting value of the isentropic efficiency for a given polytropic process can be used, as the pressure ratio approaches unity. This is known as the "polytropic"

efficiency of expanders (turbines) and compressors. Therefore, as derived in reference [14], for a compressor the polytropic efficiency is defined as:

$$\eta_{pc} \equiv \eta_{sc_{PR \to 1.0}} = \left[\frac{(\gamma-1)/\gamma}{(n-1)/n} \right] \qquad (....B.25)$$

and for an expander,

$$\eta_{pe} \equiv \eta_{se_{PR \to 1.0}} = \left[\frac{(\gamma-1)/\gamma}{(n-1)/n} \right] \qquad (....B.26)$$

For perfect gases, using equations B.18 and B.21 along with the definition of polytropic efficiencies, the following useful functions are obtained at total conditions:

For compressors -

$$\frac{T_{02}}{T_{01}} = \left(\frac{P_{02}}{P_{01}}\right)^{\left(\frac{\gamma-1}{\gamma}\right)\frac{1}{\eta_{pc}}} = \left(\frac{P_{02}}{P_{01}}\right)^{\left(\frac{R}{\bar{C}_{p2}}\right)\frac{1}{\eta_{pc}}} \qquad (....B.27)$$

and, for expanders -

$$\frac{T_{04}}{T_{05}} = \left(\frac{P_{04}}{P_{05}}\right)^{\left(\frac{\gamma-1}{\gamma}\right)\eta_{pe}} = \left(\frac{P_{04}}{P_{05}}\right)^{\left(\frac{R}{\bar{C}_{p5}}\right)\eta_{pe}} \qquad (....B.28)$$

Heat Exchangers

The thermal performance of any type of heat exchanger is usually measured by its effectiveness E , which is defined as the ratio of the heat actually transferred to the maximum amount of heat that could be transfered, i.e.

$$\varepsilon_X \equiv \frac{\dot{Q}_{actual}}{\dot{Q}_{max}} = \frac{(\dot{m}C_p)^{Cold}_{Fluid}}{(\dot{m}C_p)_{min}} \frac{[T_{03} - T_{02}]}{[T_{05} - T_{02}]} \qquad (....B.29)$$

For,

$$(\dot{m} C_p)_{\substack{cold \\ Fluid}} = (\dot{m} C_p)_{min} \qquad (....B.30)$$

$$\varepsilon_x = \frac{T_{03} - T_{02}}{T_{05} - T_{02}} \qquad (....B.31)$$

where T_{02} , T_{03} and T_{05} are represented in figure B.1.

Availability and Thermal Efficiency of Cycle

In a steady-state, steady-flow process, the maximum reversible work is obtained when the mass leaving the control volume is in equilibrium with the surroundings. This maximum reversible work or available energy is called "availability", ϕ, and is given inreference [13] as:

$$\phi = (h - h_{eq}) - T_{eq}(S - S_{eq}) + \frac{g}{g_c}(Z - Z_{eq}) + \frac{V^2}{2g_c} \qquad (....B.31a)$$

where the inlet properties are without subscript and the exit properties at equilibrium have the subscript "eq".

If the velocity entering the control volume is made to approach zero and the change in potential energy is negligible, equation B.31a becomes:

$$\phi = (h - h_{eq}) - T_{eq}(S - S_{eq}) \qquad (....B.32)$$

The entropy change ($S - S_{eq}$) for an ideal gas in a control volume is given in reference [13] as:

$$S - S_{eq} = \left(p \ln\left(\frac{T}{T_{eq}}\right) - R \ln\left(\frac{P}{P_{eq}}\right)\right. \qquad (....B.33)$$

Substituting equations (B.10) and (B.32) into equation (B.33), the following relation between availabiltity, temperature ratio and pressure ratio at a constant specific heat is obtained:

$$\phi = C_p(T - T_{eq}) + T_{eq}\left[C_p \ln\left(\frac{T_{eq}}{T}\right) - R \ln\left(\frac{P_{eq}}{P}\right)\right]$$

(....B.34)

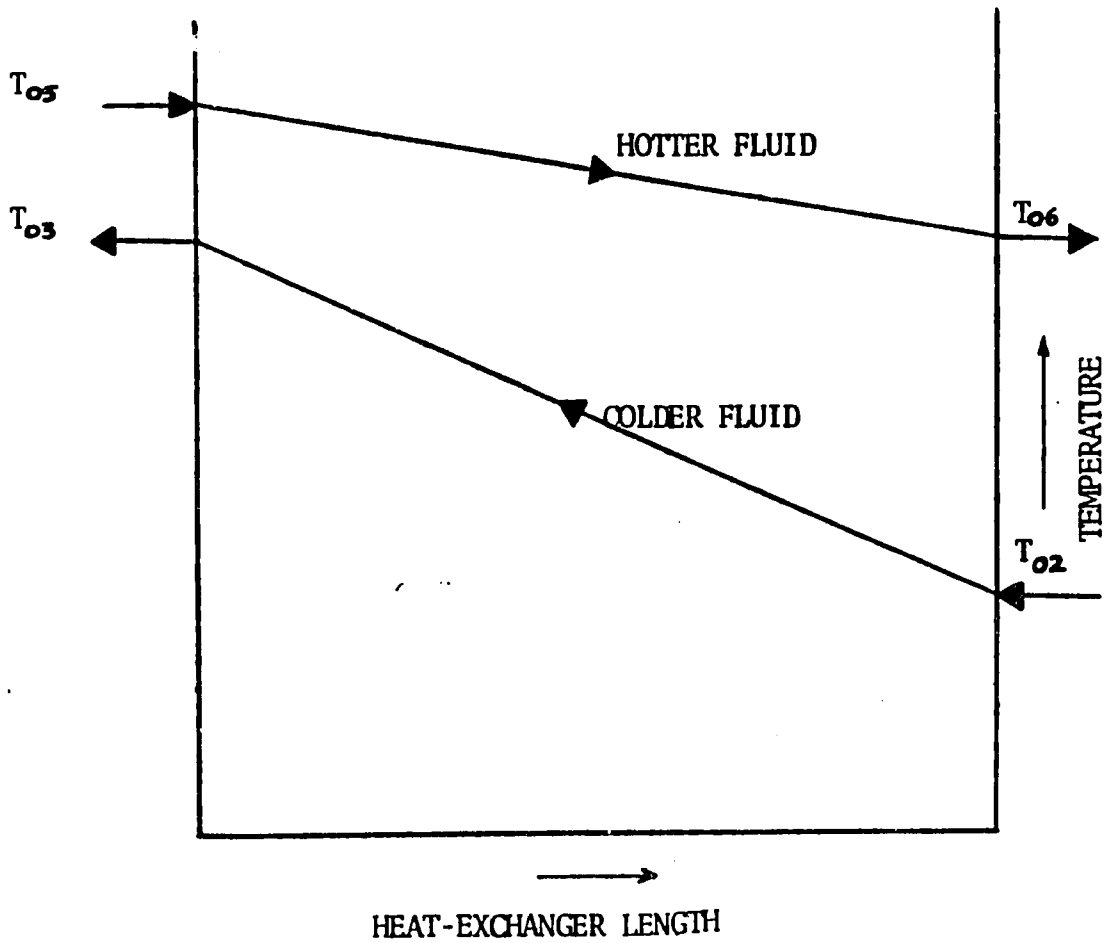

FIGURE B.1 REPRESENTATION OF TEMPERATURE DISTRIBUTION IN A COUNTERFLOW HEAT-EXCHANGER

The thermal efficiency of a cycle is defined as the ratio of the next power of the cycle to the rate of heat transferred to the system, or:

$$\eta_{th} \equiv \frac{\dot{W}_{net}}{\dot{Q}_A} \qquad (....B.35)$$

where,

$$\dot{W}_{net} \equiv \dot{W}_{expander} + \dot{W}_{compressor} \qquad (....B.36)$$

Another cycle efficiency may be defined as the ratio of the net power to the availability, , of the working fluid before it enters the energy-recovery system, or:

$$\eta_a \equiv \frac{\dot{W}_{net}}{\phi} \qquad (....B.37)$$

B.2 ANALYSIS OF THE LOW-PRESSURE CYCLE

The proposed low-pressure cycle for energy recovery from the exhaust gases of a BOF is shown schematically in figure 2.2. The oxygen used in the refining is compressed before entering the BOF. The exhaust gases from the BOF are cooled by steam injection before entering a turbine that outputs power. The exhaust gases from the turbine in turn are passed through a heat exchanger where heat is transferred from turbine exhaust gases to compressed oxygen. The hotter fluid leaving the heat exchanger then enters a waste-heat boiler which generates the steam for injection into the gas stream before it enters the turbine. The gas stream leaving the waste-heat boiler is brought to a low enough temperature for safely passing the gas into mains for distribution.

An example analysis of cycle in figure 2.1 is given as follows: The specifications given are -

$$\frac{P_{02}}{P_{01}} \equiv r_c = 3.0; \qquad (....B.38)$$

with total relative-pressure losses:

$$\sum\left(\frac{\Delta P_0}{P_0}\right) = 10\%;$$ (....B.39)

$$\frac{P_{04}}{P_{05}} = r_e = r_c\left[1 - \sum\left(\frac{\Delta P_0}{P_0}\right)\right] = 2.7;$$

$$T_{01} = 310.78^\circ K\ (100^\circ F);$$ (....B.40)

$$T_{04} = 1199.82^\circ K\ (1700^\circ F) \text{ with steam;}$$

$$T_{07} = 425^\circ K\ (150^\circ C \text{ or } 300^\circ F) \text{ injection}$$

from Appendix B, section B.5, (....B.41)

$$\dot{m}_{gas} = 42.6\ \frac{kg}{sec} \text{ and } \dot{m}_2 = \dot{m}_{O2} = 25.33\ \frac{kg}{sec};$$ (....B.42)

the compressor and turbine polytropic efficiencies are 90 % each or,

$$\eta_{pc} = 0.90 \text{ and } \eta_{pe} = 0.90;$$

(....B.43)

the effectiveness of the heat exchanger, ε_x, is given as:

$$\varepsilon_x = \frac{T_{03} - T_{02}}{T_{05} - T_{02}} = 0.75$$

(....B.44)

With these specifications, the compressor, turbine, heat exchanger and waste-heat boiler are analyzed using the equations in section B.1 to determine the power output and the steam generated for the cycle.

Oxygen Compressor

The power required to operate the oxygen compressor is determined as follows. The work done on the compressor is given, based on equation (B.13), as:

$$ {}_1W_2 = {}_1\bar{C}_{p_2} \left[T_{01} - T_{02} \right] \qquad (....B.45) $$

The exit total temperature, T_{02}, is determined using equation (B.27):

$$ T_{02} = T_{01} \left[r_c \right]^{\frac{R_{O_2}}{{}_1\bar{C}_{p_2}} \cdot \frac{1}{\eta_{pc}}} \qquad (....B.46) $$

where T_{01}, r_c and η_{pc} are as specified. The gas constant for oxygen, R_{O2}, is given by:

$$ R_{O2} = \frac{\text{Universal gas constant}}{\text{Molecular weight of } O_2} = \frac{8313.22 \text{ J/kg mole °K}}{32.00 \text{ Kg/Kg mole}} = 259.79 \text{ J/kg °K} \qquad (....B.47) $$

The specific heat, ${}_1\bar{C}_{p_2}$, is guessed to begin with, and T_{02}, is calculated from equation (B.46).

Guess ${}_1\bar{C}_{p_2}$ = 925 J/kg° K, then with R_{O2} = 259.79 J/kg K,

$$ T_{02} = 437.87°K \text{ and } {}_1\bar{T}_2 = \frac{T_{01} + T_{02}}{2} \qquad (....B.48) $$

The specific heat is now obtained from gas tables for oxygen (reference [15]) at the average temperature, ${}_1\bar{T}_2$. Iterating for ${}_1\bar{C}_{p_2}$ at the calculated ${}_1\bar{T}_2$, the following are obtained:

$$ T_{02} = 436.35^c \text{ K and } {}_1\bar{C}_{p_2} = 934.44 \text{ J/kg°K} \qquad (....B.49) $$

Therefore, the work done on the compressor is determined from equation (B.45) as:

$$_1W_2 = -117{,}341.79 \text{ J/kg} \qquad (....B.50)$$

and the power required by the compressor is:

$$_1\dot{W}_2 = \dot{m}_2 (_1w_2) = -2.97 \text{ MW} \qquad (....B.51)$$

Gas Plus Steam Turbine

The total power output by the turbine is determined as follows. The work done by the turbine is given, based on equation (B.13), as

$$_4w_5 = {}_4\bar{C}_{p5} \left[T_{04} - T_{05} \right] \qquad (....B.52)$$

The turbine exit total temperature, T_{05}, is determined using equation (B.28):

$$T_{05} = \frac{T_{04}}{\left[r_e \right]^{\frac{\bar{R}T}{{}_4\bar{C}_{p5}}} \eta_{pe}} , \qquad (....B.53)$$

where T_{04}, r_e and η_{pe} are as specified. The specific heat, C_p, for the combined steam, carbon-dioxide and carbon-monoxide stream is determined from the relation:

$$_4\bar{C}_{p5} = y_{CO} \left[\bar{C}_{pCO} \right] + y_{CO_2} \left[\bar{C}_{pCO_2} \right] + y_{H_2O} \left[\bar{C}_{pH_2O} \right] \qquad (....B.54)$$

where y, a constant, is the mass fraction of the gas and the specific heats are determined from reference [15] for the respective gases at an average temperature,

$$ {}_4\bar{T}_5 = \frac{T_{04} + T_{05}}{2} $$

(....B.55)

The gas constant after steam injection, R , is given by:

$$ R_T = \frac{\text{Universal gas constant}}{\text{Total molecular weight of gas and steam}} = \frac{8313.22\ J/kg\ mole\ ^\circ K}{22.25\ kg/kg\ mole} $$

$$ = 373.69\ J/kg\ ^\circ K, \quad (....B.55a) $$

where, the total molecular weight =

$$ y_{CO}(mwt_{CO}) + y_{CO_2}(mwt_{CO_2}) + y_{H_2O}(mwt_{H_2O}) = 22.25\ kg/kg\ mole $$

As before for the compressor, an initial value of C is guessed and iterated to obtain T from equation (B.53) and, C from equation (B.54) and the gas tables:

$$ T_{05} = 1008.17\ ^\circ K \quad \text{and} \quad {}_4\bar{C}_{p5} = 1919.51 \frac{J}{kg\ ^\circ K} $$

(....B.56)

Therefore, the work done by the turbine is determined from equation (B.52) as:

$$ {}_4W_5 = 367{,}864.77\ J/kg $$

(....B.57)

and the power output by the turbine is:

$$ {}_4\dot{W}_5 = \left[\dot{m}_{gas} + \dot{m}_{H_2O}\right]_4 w_5 $$

(....B.58)

With the mass flow rate of the injected steam, $\dot{M}_{H_2O}$, obtained from section B.5, the power output is:

$$ {}_4\dot{W}_5 = \left[42.6 + 4.67\right] \frac{kg}{s} \left({}_4w_5\right) = 17.39\ MW $$

(....B.59)

Thus the net power output as defined in equation (B.36) is determined to be:

$$ \dot{W}_{net} = 17.39 - 2.97 = 14.42\ MW $$

(....B.60)

Heat Exchanger

The temperature of the oxygen leaving the heat exchanger, T , is determined from the definition and value of effectiveness given in equations (B.31) and (B.44) respectively:

$$T_{03} = \varepsilon_x (T_{05} - T_{02}) + T_{02}$$

(....B.61)

i.e.,

$$T_{03} = 865.22^{\circ} \text{ K}$$

(....B.62)

By equating the energy lost by the hot stream to the energy gained by the cold stream, the temperature of the hot stream, T_{06}, leaving the heat exchanger is determined.

ENERGY LOST BY HOT STREAM = ENERGY GAINED BY COLD STREAM

$$[\dot{m}_{gas} + \dot{m}_{H_2O}]_5 \bar{C}_{P6} [T_{05} - T_{06}] = \dot{m}_2 \bar{C}_{P3} [T_{03} - T_{02}]$$

(....B.63)

The specific heat, ${}_2C_{P3}$, is determined from the gas tables for oxygen at -

$${}_2\bar{C}_{P3} = 1017.29 \text{ J/kg}^{\circ} \text{ K}$$

(....B.64)

All the mass-flow rates are obtained from section (B.5) and T_{05} , is obtained from equation (B.56). The specific heat, ${}_5\bar{C}_{P6}$ is initially guessed and then iterated to obtain T_{06} from equation (B.63). ${}_5C_{P6}$ is determined using mass fractions as in equation (B.54) and the specific heats of the gases determined at an average temperature,

$${}_5\bar{T}_6 = \frac{T_{06} + T_{05}}{2}$$

The specific heat and T thus obtained are:

$(\bar{C}_{p_6} = 1842.87 \text{ J/kg}^\circ \text{ K and } T_{06} = 881.36 \text{ K})$

(....B.65)

Waste-Heat Boiler

The waste-heat boiler has to fulfill two specifications:

1. $T_{07} = 425^\circ$ K, and
2. provide adequate or surplus steam in the cycle.

As energy balance on the waste-heat-boiler is performed assuming no heat loss and treating the gas and steam as separate streams in the flow from 6 to 7. Heat is transferred from the hot stream of gas and steam to the water that is pumped from a reservoir into the waste-heat boiler. The water is converted to steam as it passes through the waste-heat boiler. The mass-flow rate of steam, $\dot{m}_{steam}$, leaving the waste-heat boiler is obtained from the energy balance whereby,

ENERGY OF FLOWS ENTERING WASTE-HEAT BOILER = ENERGY OF FLOWS LEAVING WASTE-HEAT BOILER

or,

$$\dot{m}_6 h_{06}\Big]_{gas} + \dot{m}_6 h_{06}\Big]_{steam} + \dot{m}_f h_f\Big]_{A} = \dot{m}_7 h_{07}\Big]_{gas} + \dot{m}_7 h_{07}\Big]_{steam} + \dot{m}_{steam} h_{B_{steam}}\Big]_{B} \quad (....B.66)$$

For a steady-state, steady-flow process,

$$\dot{m}_6\Big]_{gas} = \dot{m}_7\Big]_{gas} = 42.6 \text{ kg/sec}$$

(....B.67)

and,

$$\dot{m}_6\Big]_{steam} = \dot{m}_7\Big]_{steam} = \dot{m}_{steam}\Big]_{B} = \dot{m}_f\Big]_{A} \equiv \dot{m}_{steam} \quad (....B.68)$$

Substituting equations (B.67) and (B.68) into equation (B.66) and rearranging, we get:

$$\dot{m}_6 h_{06}\Big]_{gas} + \dot{m}_6 h_{07}\Big]_{gas} = \dot{m}_{steam}\left[h_{B_{steam}} + h_{07_{steam}} - h_f - h_{06_{steam}}\right] \quad (....B.69)$$

and with equation (B.10), equation (B.69) can be written as:

$$(42.6)_6 \bar{C}_{p_{7_{gas}}}\left[T_{06} - T_{07}\right] = \dot{m}_{steam}\left[h_{B_{steam}} + h_{07_{steam}} - h_f - h_{06_{steam}}\right] \quad (....B.70)$$

The average temperature,

$$_6\bar{T}_7 = \frac{T_{06} + T_{07}}{2} = 653.18^{\circ}K$$

and the gas tables are used to determine the specific heat of the gas stream $_6\bar{C}_{p_7}$ on a mass fraction basis as:

$$_6\bar{C}_{p7} = y_{CO}(\bar{C}_{pCO}) + y_{CO_2}(\bar{C}_{pCO_2})$$
$$= 420.74 \ J/kg\,^{\circ}K \qquad (....B.71)$$

The enthalpies of steam in equation B.70 are determined from steam tables for the respective temperatures and pressures:

$$h_{06\,Steam} = 3705.40 \ kJ/kg$$

at

$$T_{06} = 881.36 \ K$$

and a partial pressure of steam,

$$p_{06} = 0.07 \ MPa,$$

where p_{06} is determined as follows:

$$P_{06} = y_{H2O} P_{05} \qquad (....B.72)$$
$$= y_{H2O}\left(\frac{P_{04}}{2.7}\right)$$
$$= y_{H2O}\left(\frac{3(P_{atm})}{2.7}\right)$$
$$= 0.6175\left(\frac{3(14.7)}{2.7}\right)$$

$$\text{or, } P_{06} = 10.09 \ psi. \simeq 0.07 \ MPa \qquad (....B.73)$$

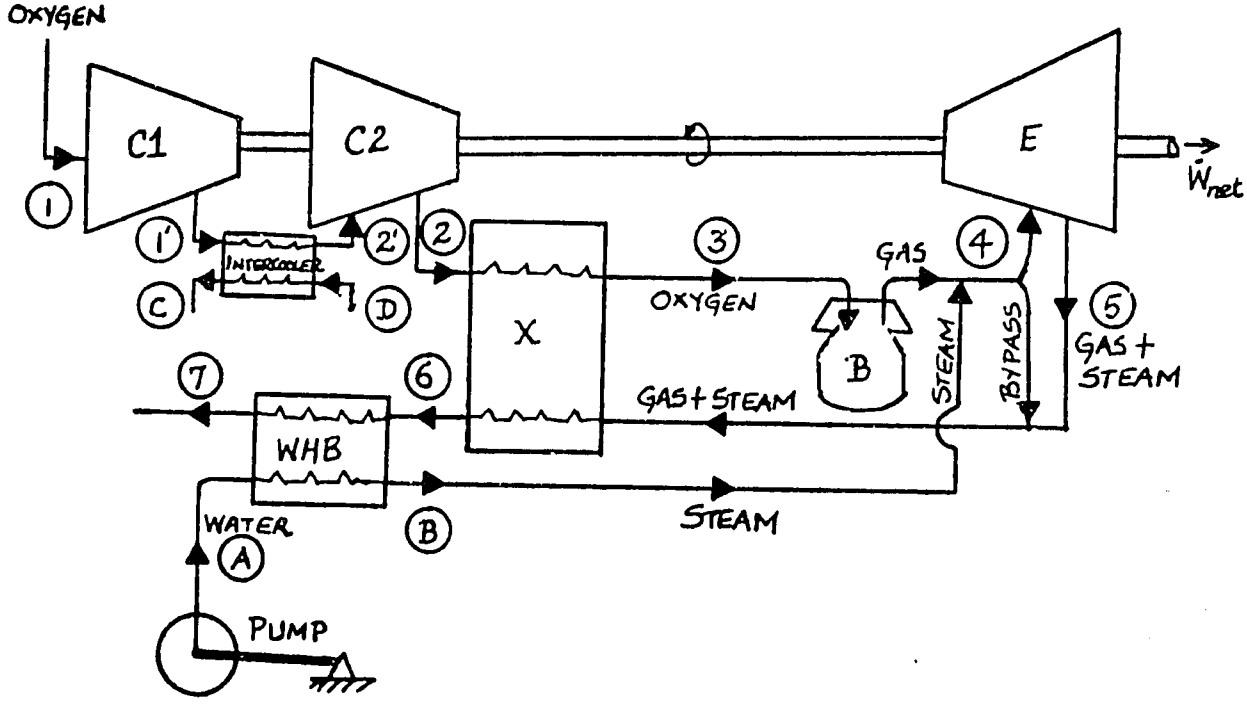

FIGURE B.2 INTERCOOLED COMPRESSOR CYCLE FOR ENERGY-RECOVERY FROM EXHAUST GASES OF THE BASIC OXYGEN FURNACE.

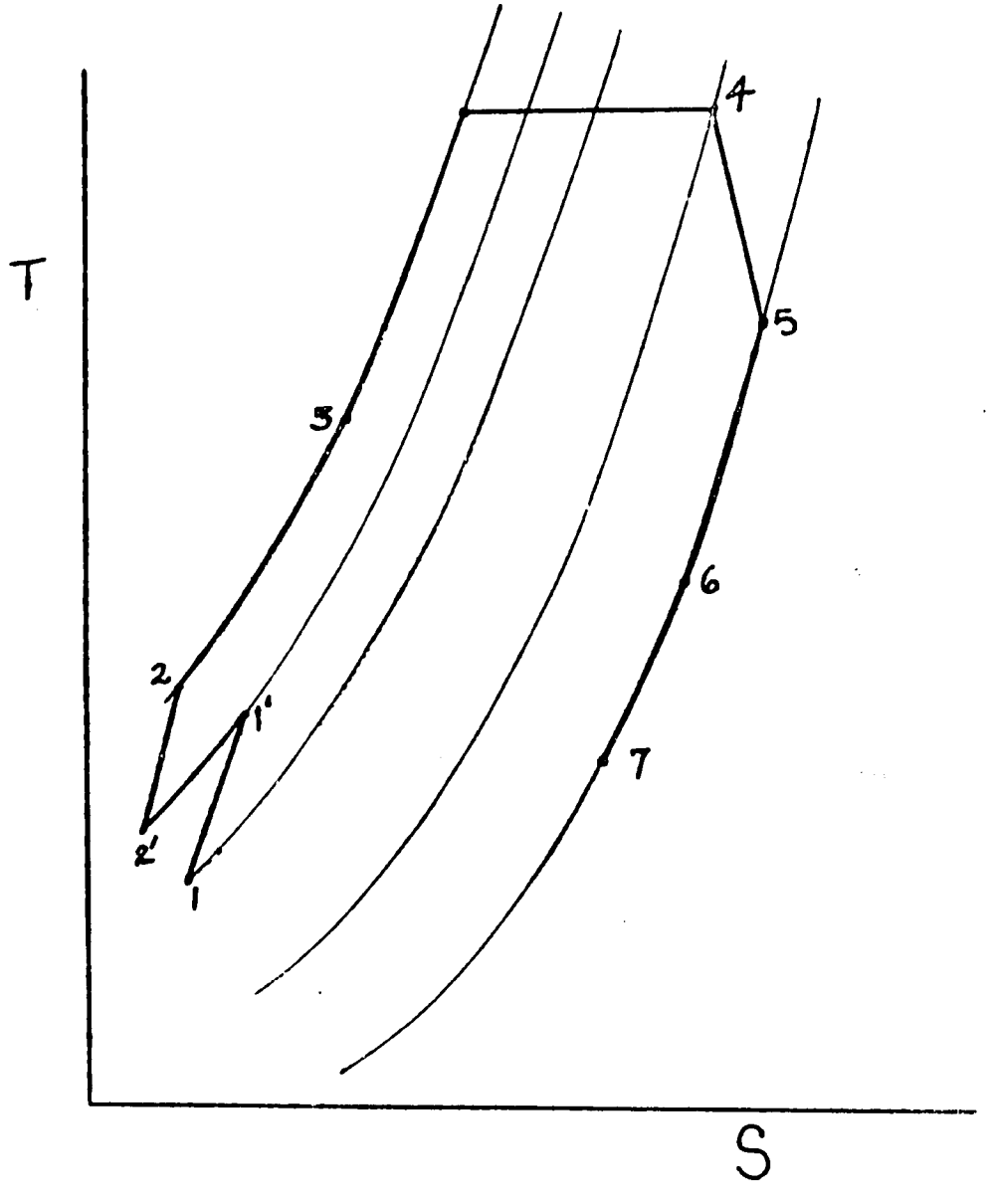

FIGURE B.3 TEMPERATURE-ENTROPY DIAGRAM FOR INTERCOOLED COMPRESSOR ENERGY-RECOVERY CYCLE OF FIGURE B.2 .

$$h_f = 104.89 \text{ kJ/kg at } T_f = T_{0A} = 298^\circ \text{K}$$

(temperature of reservoir is assumed to be 77 F = 25 C = 298° K) and, P_f = 3 atm;

$h_{07_{steam}}$ = 2782 kJ/kg at T_{07} = 425° K and a partial pressure, p_{07} ,

where, $p_{07} = p_{06}$ = 0.07 MPa;

$$h_{B_{steam}} = 2725 \text{ kJ/kg at } T_{0B} = 408^\circ \text{ K and } P_{0B} = 3 \text{ atm,}$$

where T_{0B} = 408 K (= T_{sat}) is the minimum temperature required to obtain steam at a pressure of 3 atm.

Therefore, substituting the values of specific heat, enthalpies and temperatures into equation B.70 and solving for $\dot{m}_{steam}$, we get:

$$\dot{m}_{\substack{steam \\ WHB}} = \frac{(42.6)\frac{kg}{sec}\ 420.74\ J/kg\,^\circ K\ [881.36 - 425]^\circ K}{[2725 + 2728 - 104.89 - 3705.40]\ KJ/kg}$$

$$= 4.28\ kg/sec \qquad (....B.74)$$

The mass-flow rate of steam leaving the waste-heat boiler is slightly greater than the mass-flow of steam required to reduce the temperature of BOF exhaust gases before entering the turbine.

B.3 FEASIBILITY STUDY ON INCORPORATING AN INTERCOOLED COMPRESSOR IN THE ENERGY RECOVERY CYCLE.

Introduction

It can be seen in equation (B.45) that the compression work is directly proportional to the change in absolute temperatures. The exit temperature, T_{02} , increases with increasing pressure ratio as seen in equation (B.46) for an isentropic process. Hence, the work required to accomplish a larger pressure ratio compression will be greater than the work required for lower pressure ratio compression. By cooling the compressed gas between the stages or groups of stages, will decrease the work required for larger-pressure-ratio compression and the net output increases for the cycle. It was therefore, attractive to consider one intercooler based on a practical, economic limit on the number of intercoolers and the possibility of increasing cycle power output. The intercooled-oxygen-compressor cycle is shown in figure B.2 and represented on a T-S diagram in figure B.3.

Analysis of the Intercooled Compressor

For a specified total compression pressure ratio of three, the pressure ratio across each compressor is specified to be equal. Therefore, with:

$$\frac{P_{02}}{P_{01}} = \frac{P_{01}'}{P_{01}} \cdot \frac{P_{02}}{P_{01}'} = \frac{P_{01}'}{P_{01}} \cdot \frac{P_{02}}{P_{02}'} = 3 \qquad (....B.75)$$

where it is specified that P_{01}' = P_{02}' and are total pressures at designated stations ① and ② in figure B.2, each of the pressure ratios are:

$$\frac{P_{01}'}{P_{01}} = \frac{P_{02}}{P_{02}'} = 1.732 \qquad (....B.76)$$

The power required by the compressor, C , is determined just as for the oxygen compressor in section B.3 of this appendix. As specified before,

$$\eta_{pc1} = 0.90,$$
$$T_{01} = 310.78^{\circ}\ K,$$
$$\dot{m}_{c1} = 25.33\ kg/sec,$$

oxygen is the working fluid and from equation (B.47),

$$R_{02} = 259.79\ J/kg^{\circ}\ K.$$

Therefore, T_{01}' is obtained from equation (B.46) for a pressure ratio, r_c = 1.732 as:

$$T_{01}' = 310.78^{\circ}K\ [1.732]^{\frac{259.79}{{}_1\bar{C}_{p1}'}}\ \frac{1}{0.90} = 368.57^{\circ}K \qquad (....B.77)$$

for,

$${}_1\bar{C}_{p1'} = 929.72\ J/kg^{\circ}\ K$$

The compressor work is then determined from equation B.45 as:

$${}_1W_1' = -53,728.52\ J/kg \qquad (....B.78)$$

and the power required by the compressor C1 is:

$${}_1\dot{W}_1' = \dot{m}_{c1}\,({}_1W_1') = -1.36\,MW \qquad (....B.79)$$

It is assumed that the temperature of the oxygen leaving the intercooler, T_{02}', is equal to the temperature

of the oxygen entering the first compressor, (T_{01} = 310.78° K.

Hence, with

$$T_{02'} = T_{01}$$

and equal pressure ratios across compressors C2 and C1, the power required by each compressor is equal. That is,

$$_{1}\dot{W}_{1'} = {}_{2'}\dot{W}_{2} = -1.36\,MW \qquad (....B.80)$$

and therefore, total compression power required is:

$$_{1}\dot{W}_{2_{IC}} = 1.36 + (-1.36) = -2.72\,MW \qquad (....B.81)$$

Conclusions of Study

Comparing equations (B.81) and (B.51), it is seen that intercooling does reduce the power required for compression by 8.4%, that is:

$$\frac{|{}_{1}\dot{W}_{2}| - |{}_{1}\dot{W}_{2_{IC}}|}{|{}_{1}\dot{W}_{2}|} = \frac{2.97 - 2.72}{2.97} = 0.084 \qquad (....B.82)$$

or,

$$1 - \left[\frac{{}_{1}\dot{W}_{2_{IC}}}{{}_{1}\dot{W}_{2}}\right] = 0.084 \qquad (....B.83)$$

But intercooling increases net power of the cycle by only 1.7%, for the same turbine power output of 17.39 MW:

$$\frac{\dot{W}_{net_{IC}} - \dot{W}_{net}}{\dot{W}_{net}} = \frac{[{}_{4}\dot{W}_{5} + {}_{1}\dot{W}_{2_{IC}}] - [{}_{4}\dot{W}_{5} + {}_{1}\dot{W}_{2}]}{{}_{4}\dot{W}_{5} + {}_{1}\dot{W}_{2}} = \frac{[17.39 - 2.72] - [17.39 - 2.97]}{17.39 - 2.97} \qquad (....B.84)$$

$$= 0.0173 \simeq 1.7\%$$

The percent power gain is low because the magnitude of the compressor work in this study is not large enough to significantly affect the change in net power output betwen the cycle being intercooled and not intercooled. This can be seen from equation (B.89) which is derived as follows:

$$\dot{W}_{net_{IC}} = 4\dot{W}_5 + {}_1\dot{W}_{2IC} \qquad (....B.85)$$

$$\dot{W}_{net} = 4\dot{W}_5 + {}_1\dot{W}_2 \qquad (....B.86)$$

or, substituting W from equation (B.83) into equation (B.85) and rearranging we get:

$$\frac{\dot{W}_{net_{IC}}}{4\dot{W}_5} = 1 - \left(\frac{0.916\left|{}_1\dot{W}_2\right|}{4\dot{W}_5}\right) \qquad (....B.87)$$

$$\dot{W}_{net} = 1 - \left(\frac{\left|{}_1\dot{W}_2\right|}{4\dot{W}_5}\right) \qquad (....B.88)$$

and therefore,

$$\dot{W}_{net_{IC}} - \dot{W}_{net} = 0.084\left|{}_1\dot{W}_2\right| \qquad (....B.89)$$

So an intercooled compressor will add investment and operating costs to cycle design without significantly increasing the net power output and it is concluded that an intercooled compressor is not feasible for the specified cycle.

B.4 STEAM INJECTION AND MASS-FLOW RATES

Steam is injected into the mainstream of exhaust gases from the pressurized BOF before the flow enters the power turbine. This is done to lower the temperature of the BOF exhaust gases to a value that can be tolerated by typical materials of uncooled blades and nozzles of the gas turbine. The added mass-flow due to the steam, produces an increase in power output from the turbine as discussed in reference [16].

The mass-flow rate of the steam required to lower the temperature of BOF exhaust gases from 1588 K (2400 F) to 1199 K (1700 F) for an average m is calculated as follows. A control volume, figure B.4, is isolated within the exhaust gas pipe before the power turbine and a steady-state, steady-flow analysis is performed. Assuming an adiabatic flow, zero change in potential energy and with no shaft work, an energy balance based on the first law of thermodynamics (equation (B.1)) is given by:

$$\dot{m}_{\substack{steam\\in}} h_{g_{in}} + \dot{m}_{\substack{gas\\in}} h_{\substack{gas\\in}} = \dot{m}_{\substack{steam\\out}} h_{g_{out}} + \dot{m}_{\substack{gas\\out}} h_{\substack{gas\\out}} \qquad (....B.90)$$

From continuity and SSSF,

$$\dot{m}_{\substack{steam\\in}} = \dot{m}_{\substack{steam\\out}} = \dot{m}_{\substack{steam\\required}} \qquad (....B.91)$$

and,

$$\dot{m}_{\substack{gas\\in}} = \dot{m}_{\substack{gas\\out}} \equiv \dot{m}_{gas} = 42.6\ kg/sec. \qquad (....B.92)$$

Substituting equations (B.91) and (B.92) into equation (B.90) and rearranging we get:

$$\dot{m}_{\substack{steam\\required}} = \frac{\dot{m}_{gas}\left[h_{gas} - h_{gas_{in}}\right]}{\left[h_{g_{in}} - h_{g_{out}}\right]_{steam}} \qquad (....B.93)$$

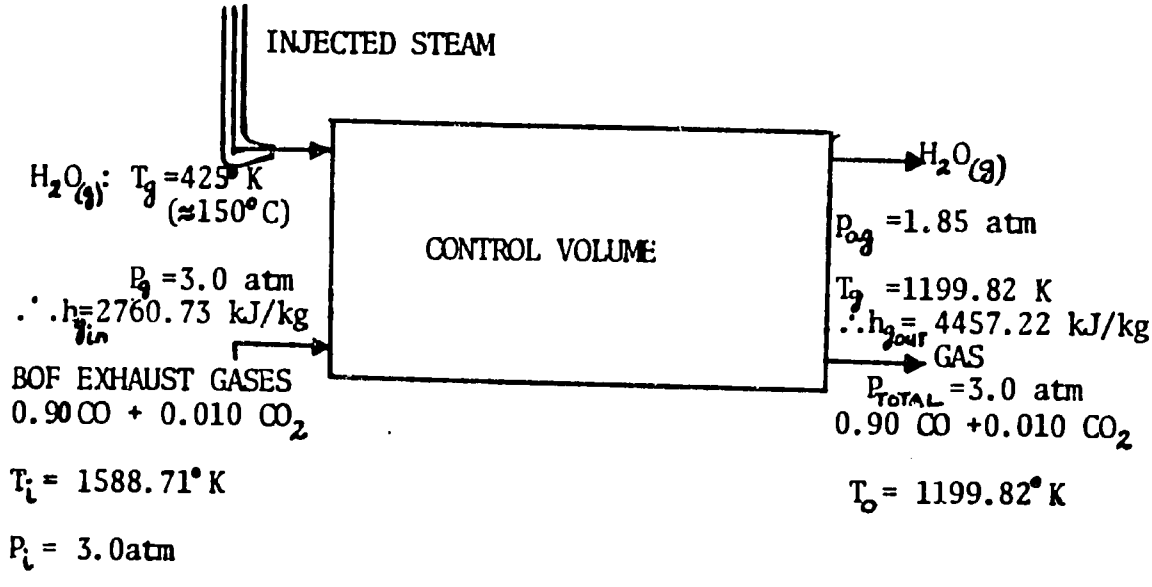

FIGURE B.4 STEAM INJECTION INTO BOF EXHAUST GASES.

HEAT LOSSES ARE NEGLECTED.

The enthalpies of steam are obtained from the gas tables at specified conditions in figure B.4. The partial pressure, P_{ag} of the steam exiting the control volume is determined using Dalton's law of partial pressures:

$$P_{ag} = y_1 P_{TOTAL}$$

(....B.94)

where y_1 is the mass fraction of steam in the flow, or:

$$P_{ag} = 0.6175 \times (3.0) \text{ atm.} = 1.85 \text{ atm.}$$

(....B.95)

The change in enthalpies of the BOF exhaust gases is given in terms of absolute temperatures and specific heat using equation (B.10). Therefore, from equation (B.93):

$$\dot{m}_{\substack{steam \\ required}} = \frac{42.6 \text{ kg/s } 478.24 \text{ J/kg°K } [1199.82 - 1588.71]\text{°K}}{[2760.73 - 4457.22] \times 10^3 \text{ J/kg}}$$

$$= 4.67 \text{ kg/s},$$

(....B.96)

where,

$$\bar{C}_{P_{gas}} = y_{CO}[\bar{C}_{P_{CO}}] + y_{CO_2}[\bar{C}_{P_{CO_2}}] = 478.24 \text{ J/kg°K at}$$

$$\bar{T}_{gas} = \frac{1199.82 + 1588.71}{2} \simeq 1394\text{°K}$$

Mass-Flow Rate

The average mass-flow rate for a 80-ton BOF at the Helwan plant in Egypt is obtained from M. Ahdab as:

$$\dot{m}_{gas} = 42.6 \text{ kg/sec}$$

(....B.97)

The mass-flow-rate of oxygen is determined as follows: The percentage of CO and CO in the BOF exhaust gases is obtained from reference [2] as 90% CO and 10% CO_2 by weight. Therefore,

$$0.55n\,O_2 + nC \rightarrow 0.90\,nCO + 0.10n\,CO_2$$

(....B.98)

where, n = number of moles of the exhaust gas. The mass-flow rate of O is given by:

$$\dot{m}_{O_2} = \dot{n}_{O_2} MWt_{O_2}$$

(....B.99)

where,

$\dot{n}_{O_2}$ ≡ number of moles of O_2 per second, and
MWt_{O_2} ≡ molecular weight of O_2.

From equation (B.98),

$$(\dot{n}_{O_2} = 0.55\ \dot{n})$$

(....B.100)

where,

$$\dot{n} \equiv \frac{\dot{m}_{gas}}{MWt_{gas}} = \frac{42.6\ Kg/s}{[0.90(28)+0.10(44)]\ Kg/mole} = 1.44\ \frac{mole}{sec}$$

and

$$\dot{n}_{O_2} = 0.55(1.44) = 0.79\ \frac{mole}{sec}$$

(....B.101)

Substituting equation (B.101) and

$$MWt_{O_2} = 32\ kg/mole$$

into equation (B.99),

$$\dot{m}_{O_2} = 25.33\ kg/sec)$$

(....B.102)

For the bulk flow of a fluid of static density ρ , moving

through a cross sectional area A, the mass-flow rate, $\dot{m}$, is given by:

$$\dot{m} = \rho V A \qquad (....B.103)$$

where, V is the component of fluid velocity normal to the cross-sectional area A. From reference [2], chapter 9, the typical peak volume flow rate, VA, for a 80-ton BOF is obtained as:

$$VA = 6000 \text{ ft}^3 \text{/min)} \qquad (....B.104)$$

Using the perfect gas law, the static density is given by:

$$\rho = \frac{P}{RT} \qquad (....B.105)$$

where,

P = (Pressure of oxygen from reservoir) x Pressure ratio = 149.7 x 3.0 lbf/in^2 ;

$R = R_{O_2}$ = 259.79 J/kg° K; and

$T = T_{03}$ = 865.22° K [from equation (B.62)]

Therefore, in equation (B.103),

$$\dot{m}_{O_2\,peak} = \frac{149.7 \times 3.0 \frac{lbf}{in^2}\left(1.44 \frac{in^2}{ft^2}\right) 6000\, ft^3/min \cdot min/60 sec}{259.79 \frac{J}{kg\,°K}\left(865.22°K\right)\left(0.7376\right)\frac{ft-lbf}{J}} = 39.0\ kg/sec \qquad (....B.106)$$

Solving for $\dot{n}$ from equations (B.99) and (B.100) we get:

$$\dot{n}_{peak} = \frac{\dot{m}_{O2\ peak}}{0.55\ MWt_{O2}} = 2.22\ \frac{mole}{sec}$$

(....B.107)

and therefore the peak gas flow rate is determined as:

$$\dot{m}_{gas_{peak}} = (\dot{n}_{peak})\ MWt_{gas}$$
$$= 65.60\ kg/sec.$$

(....B.108)

Variation of Mass-Flow Rate with Time

The mass-flow rate of the BOF exhaust gases fluctuates during the oxygen-blowing time of approximately 20 minutes. The peak gas flow obtained in equation (B.104) is assumed to occur at half the oxygen-blow time and even with several BOF s operating in a plant like the one at Helwan, it is found that a zero flow condition through the turbine may not be avoided during a BOF operating cycle of 45 minutes. It seemed necessary to avoid the zero-flow condition to atleast obtain the power necessary for continued running of the oxygen compressor. To prevent a zero-flow condition through the turbine during any part of the 45minute cycle, the time between BOF start-ups, Δt_s, , cannot be less than $\Delta t_o/(n-1)$, where Δt_o is the time between the end of the oxygen blow (or exhaust gas production) and the 45minute cycle and n is the number of furnaces. For the Helwan plant with three 80-ton BOFs (reference [17]), it is found that at:

$$\Delta t_s = \Delta t_0/(n-1)$$

(....B.109)

a zero-flow conditi on could exist at 45 minutes or just before BOF 1 starts up again (see figure B.5). Therefore, a Δt_s = 15minutes is specified and figure B.6 is obtained. However, there is a tremendous variation in mass-flow rate of the gas entering the turbine and even though figure B.6 shows a minimum flow of 20 kg/sec, based on the assumed blowing profile in

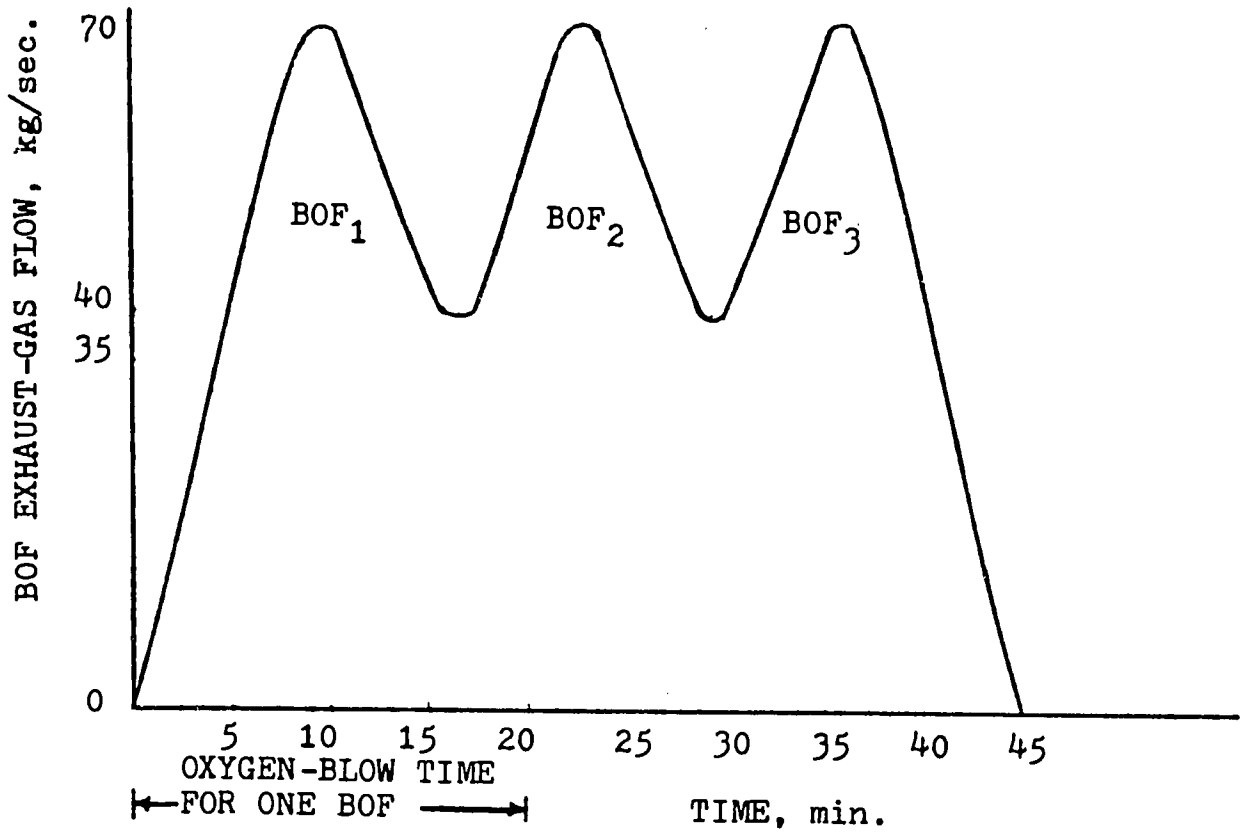

FIGURE B.5 BOF EXHAUST-GAS FLOW FOR $\Delta t_{start\ up}$ = 12.25mins.

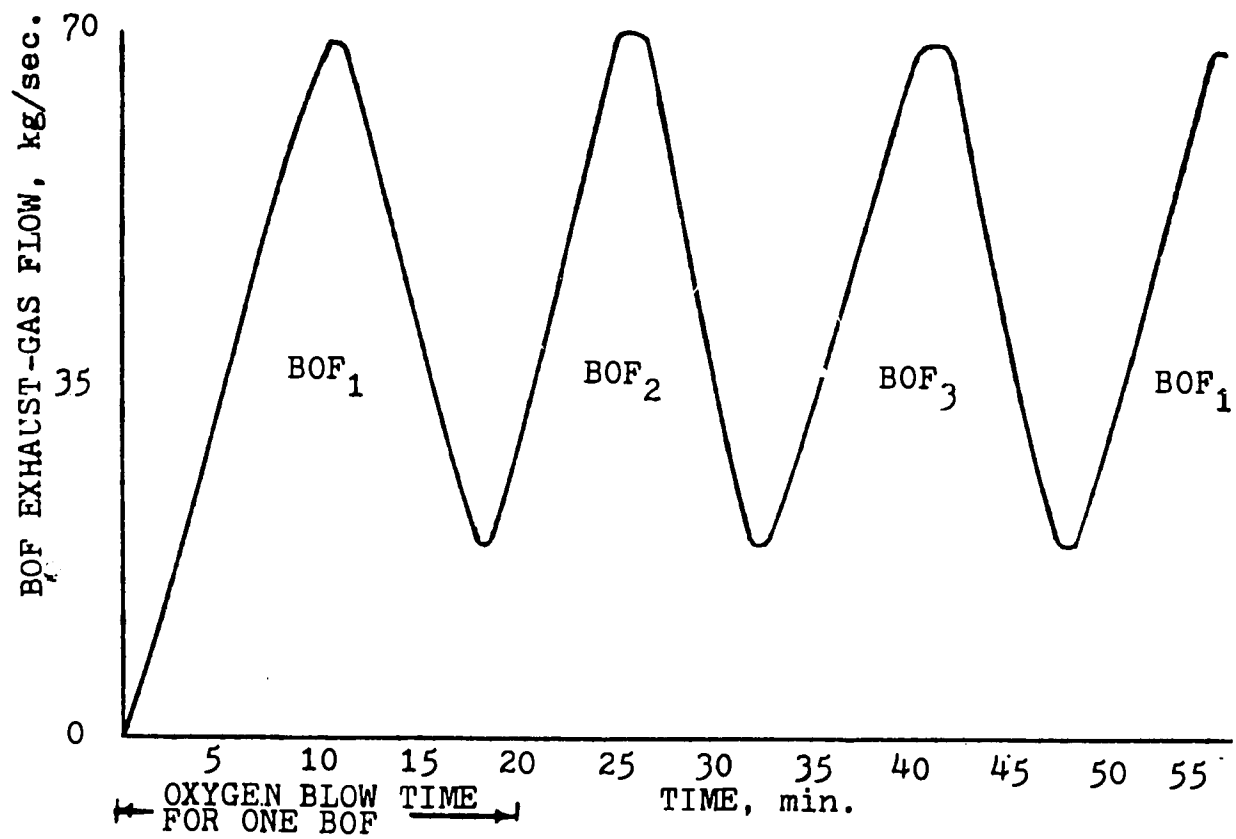

FIGURE B.6 BOF EXHAUST-GAS FLOW FOR $\Delta t_{start\ up}$ = 15mins.

practice, a zero-flow condition may not be avoided. Therefore, the specification of Δt_5 could be relaxed to 5minutes to avoid a high peak flow rather than to avoid a zero-flow condition (see chapter 3, section 3.3)

B.5 CALCULATION OF OPTIMUM PRESSURE RATIO FOR MAXIMUM POWER OUTPUT

The pressure ratio which gives maximum specific power in the energy-recovery cycle is calculated based on the specifications, gas constants and specific heats from section B.3. The specific power is defined in reference [14] as:

$$\dot{W}' \equiv \frac{\dot{W}_{net}}{\dot{m}_2 \bar{C}_{p2} T_{01}} = \left[\frac{{}_4\dot{m}_5 \, {}_4\bar{C}_{p5}}{\dot{m}_2 \, {}_1\bar{C}_{p2}}\right] E_1 T' - C \qquad (....B.110)$$

where,

$$E_1 \equiv 1 - \left\{\left\{1 - \sum\left(\frac{\Delta P_D}{P_D}\right)\right\} r\right\}^{-\left(\frac{R_T}{{}_4\bar{C}_{p5}}\right)\eta_{pe}} , \qquad (....B.111)$$

$$T' \equiv \frac{T_{04}}{T_{01}} , \qquad (....B.112)$$

$$C \equiv \left\{ r^{\left(\frac{R_{02}}{{}_1C_{p2}}\right)/\eta_{pc}} - 1 \right\} \qquad (....B.113)$$

and,

$${}_4\dot{m}_5 = (42.6 + 4.67)\,kg/sec = 47.3\,kg/sec \qquad (....B.114)$$

Therefore,

$$\dot{W} = 3.83\left\{1-\left[(1-0.10)r\right]^{-0.1752}\right\}\left[\frac{1199.82}{310.78}\right] - \left[r^{0.3089} - 1\right]$$

$$= 14.79\left\{1-(0.90r)^{-0.1752}\right\} - r^{0.3089} + 1 \qquad (....B.115)$$

At maximum specific power:

$$\frac{d\dot{W}'}{dr} = 0 = 2.6395r^{-1.1752} - 0.3089^{-0.6911} \qquad (....B.116)$$

from which,

$$r_{opt} \approx 84 .$$

This pressure ratio is generally unrealistic and impractical in a cycle with the level of mass-flow rates involved. In practice, the component efficiencies obtainable would decrease as pressure ratios increased, but the optimum pressure ratio would still not fall into a practicable range.